THESIS FOR THE DEGREE OF DOCTOR OF PHILOSOPHY

Micro-scale Platforms for Investigations of Biological Structures

ANNA A. KIM

Department of Chemistry and Chemical Engineering
CHALMERS UNIVERSITY OF TECHNOLOGY
Göteborg, Sweden 2016

Micro-scale Platforms for Investigations of Biological Structures
ANNA A. KIM

ISBN: 978-91-7597-499-6

Doktorsavhandlingar vid Chalmers Tekniska Högskola
Ny serie nr 4180
ISSN: 0346-718X

Department of Chemistry and Chemical Engineering
Chalmers University of Technology
SE-412 96 Göteborg
Sweden
Telephone: +46-(0)31 772 1000

Front cover image: ”From design to device”

Printed by Chalmers Reproservice
Göteborg, Sweden 2016

Micro-scale Platforms for Investigations of Biological Structures

ANNA A. KIM
Department of Chemistry and Chemical Engineering
Chalmers University of Technology

Abstract

This thesis describes the development of innovative micro-scale platforms as a means to address the current challenges within the field of cell biology, and to provide an interface between miniaturized analytical technology and experimental systems for the life sciences. The work includes an analytical platform for rapid assessment of the viability of adherent single cells; a surface patterning strategy for investigations of cell-to-cell communication via protrusions; a versatile microfluidic probe in SU-8 hard-polymer, and a microfabricated millimeter-wave measurement system for the identification and characterization of niosome (non-ionic surfactant vesicle) constituents, which is operated in a label-free, non-invasive manner.

One of the major challenges in cell biology is to understand the heterogeneity of cells, *i.e.*, cells of the same species and in the same local environment can differ dramatically. Recent evidence suggests that these differences in individual cells can affect the development, health and function of the entire cell population, and for this reason, single-cell studies have become increasingly important. However, there remains a need of instrumentation for efficient analytical investigations on single cells in adherent cultures and tissue slices.

My thesis addresses some of the research problems that life scientists encounter in single-cell experiments, and suggests novel analytical devices and protocols that provide efficient solutions to these problems. One of them is a protocol for the rapid determination of the viability of individual mammalian cells in adherent cell cultures, utilizing a microfluidic device for selective perfusion of targeted cells (Paper I).

I also introduce micropatterned cytophobic polymer (Teflon AF) on glass as cell culture substrate, which exhibits differential adhesion properties with respect to biological cells. This enabled the analysis of spatially separated cells in terms of their ability to establish interconnections by reaching out to other cells via protrusions, guided by the pre-determined surface pattern. Applying a microfluidic device for selective perfusion of single cells grown on these substrates allowed for examination of the chemical communication between interconnected pairs of cells (Paper II).

In Paper III, a facile process for fabrication of free-standing microfluidic devices in a photo-patternable hard-polymer (SU-8) is reported. This constitutes a major, necessary step towards large-scale fabrication of diversely functionalized single-cell superfusion devices with high potential in drug screening and diagnostics.

Finally, in Paper IV, a concept for an open-volume dielectric spectroscopy platform based on millimeter-wave technology, developed for label-free identification and characterization of niosome constituents, is presented. The microfabricated platform creates new opportunities for analyzing and characterizing the compositional variances in niosome membranes in the context of drug delivery.

Keywords: microfabrication, Teflon® AF, cell protrusions, cell-to-cell connections, single-cell viability, hydrodynamic flow confinement, SU-8, free-standing probes, millimeter-waves, non-ionic surfactants.

List of Publications

This thesis is based on the work presented in the research papers below, which are referred to as Paper I–IV in the text.

I Zhang, H.*, **Kim, A.***, Xu, S., Jeffries, G. D. M., and Jesorka, A. (2015) Cellular communication via directed protrusion growth: critical length-scales and membrane morphology. *Nano Communication Networks*, 6(4), 178–182. (*These authors contributed equally to this work).

II Xu, S., **Kim, A.**, Jeffries, G. D. M., and Jesorka, A. (2014) A rapid microfluidic technique for integrated viability determination of adherent single cells. *Analytical and bioanalytical chemistry*, 407(5), 1295–1301.

III **Kim, A. A.**, Kustanovich, K., Baratian, D., Ainla, A., Shaali, M., Jeffries, G. D. M., and Jesorka, A. SU-8 free-standing microfluidic probes. *Manuscript*.

IV Rodilla, H.*, **Kim, A. A.***, Jeffries, G. D. M., Vukusic, J., Jesorka, A., and Stake, J. (2016) Millimeter-wave sensor based on a $\lambda/2$-line resonator for identification and dielectric characterization of non-ionic surfactants. *Scientific reports*, 6. (*These authors contributed equally to this work).

Contribution Report

My contribution to the papers appended in this thesis is as follows:

I I contributed to the fabrication of the substrates, the writing of the paper and the discussion of the results.

II I contributed to the writing of the paper, data evaluation and the discussion of the results.

III I contributed to the planning, the development of the microfabrication process and the experiments. I wrote most of the paper.

IV I contributed to the design and development of the platform, the experiments, the writing of the paper and the discussion of the results.

Other papers and publications

The following papers and publications are not appended to the thesis, either due to contents overlapping of that of appended papers, or due to contents not related to the thesis.

I Nekimken, A. L., Fehlauer, H., **Kim, A. A.**, Kjono, S. N., Ladpli, P., Memon, F., Gopisetty, D., Sanchez, V., Goodman, M. B., Pruitt, B. L., Krieg, M. Pneumatic stimulation of *C. elegans.* mechanoreceptor neurons in a microfluidic trap. *Submitted.*

II **Kim, A. A.**, Rodilla, H., Jeffries, G. D. M., Vukusic, J., Stake, J., and Jesorka, A., (2015, October) Label-free millimeter-wave sensor for investigations of biological model membrane systems. In *19th International Conference on Miniaturized Systems for Chemistry and Life Sciences (μTAS)*, Chemical and Biological Microsystems Society, ISBN 978-0-9798064-8-3.

III Rodilla, H., **Kim, A.**, Vukusic, J., Jeffries, G. D. M., Vukusic, K., Jesorka, A., and Stake, J. (2014, September) Millimetre-wave dielectric spectroscopy for cell analysis. In *39th International Conference on Infrared, Millimeter, and Terahertz waves (IRMMW-THz)*, 1–2, IEEE, ISSN 2162-2027.

IV Jeffries, G. D. M., **Kim, A. A.**, Kustanovich, K., Jesorka, A. (2016) Open volume microfluidic probes, *Compendium of In Vivo Monitoring in Real-Time Molecular Neuroscience*, vol.2, World Scientific Press.

Contents

Chapter 1. Introduction

1 Introduction

The need to experimentally address biological structures at their size-scale has led to the rapid development of microsystems for life science applications, facilitated by the recent advancements in miniaturization technology. If we consider some of the important size scales of biological entities, we find that they range from nanometers to micrometers. For example, the DNA double helix is 2 nm wide, the cell membrane is 5 nm thick, a virus particle is 20 to 400 nm, organelles range from 100 nm to around 1 μm, and a typical eukaryotic cell is between 10 and 100 μm (see Figure 1.1). Advances in material science and nano- and microfabrication processes have enabled the development of devices that can probe and manipulate biological structures at this size scale, ranging from patterned surfaces to integrated systems for biological and biomedical assays.

In this context, we have developed a platform for investigating molecular transport phenomena in a network of natural intercellular connections. A previously reported method employed a micro-needle manipulation protocol for man-made network architectures involving biological cells, however, this work presented a high risk of cell damage [1]. We were interested in the possibility of controlling a natural network formation between adherent cells. By combining micropatterning of a cytophobic polymer (Teflon AF) for fabricating substrates capable of directing the growth of cell protrusions and a superfusion device for local solution delivery, we established a platform for investigating natural cellular connections. This platform can further advance fundamental studies of cell-to-cell communication capabilities in generated cellular networks, as well as chemical species and organelle exchange between biological cells.

The recent increase in the interest of single-cell studies has led to the need for suitable protocols and instrumentation. For this reason, we decided to address the necessity for assessing the viability of selected individual cells in conjunction with other experimental procedures. We employed a free-standing superfusion device for local delivery of viability agents, without adversely affecting the surrounding cells.

Considering the limited material choices for the currently available free-standing microfluidic probes, we developed a microdevice fabrication route using a rigid photo-patternable material. This process, based on a thermo-responsive sacrificial layer, enables a dry mechanical release of the final microstructures. We demonstrate three practical implementations: i) a microfluidic probe, ii) a probe with integrated thin-film electrodes and iii) a probe with perforated walls for microdialysis.

Label-free techniques are of great interest in life science studies, notably within investigations of biological and biomimetic membrane systems, since chemical modifications and the presence of dyes could alter physiological functions on a molecular level. Dielectric spectroscopy in different frequency regions is a set of label-free techniques that could provide structural and functional information on tissues, cells, and cell components. The sub-millimeter-wave region has remained to a large extent unexplored in life science applications, but it holds potential for new insights into biological processes and structures. We developed a flexible and non-invasive on-wafer measurement platform in the millimeter-wave range, with potential for advancing towards sub-millimeter-waves.

Selected biological structures, for which the new micro-scale platforms were developed, are introduced in Chapter 2. Chapter 3 provides a background to commonly used microfabrication techniques and Chapter 4 highlights the materials employed in the work that led to this thesis. An overview over the concepts of the technological advances, relevant to this work, is presented in Chapter 5. Finally, the work is summarized in Chapter 6 and concluded in Chapter 7.

The intention of the investigations presented in this thesis was to advance the research possibilities for the life sciences. The novel micro-scale platforms presented here enhance the technological foundation for monitoring, manipulating and analyzing complex biological structures.

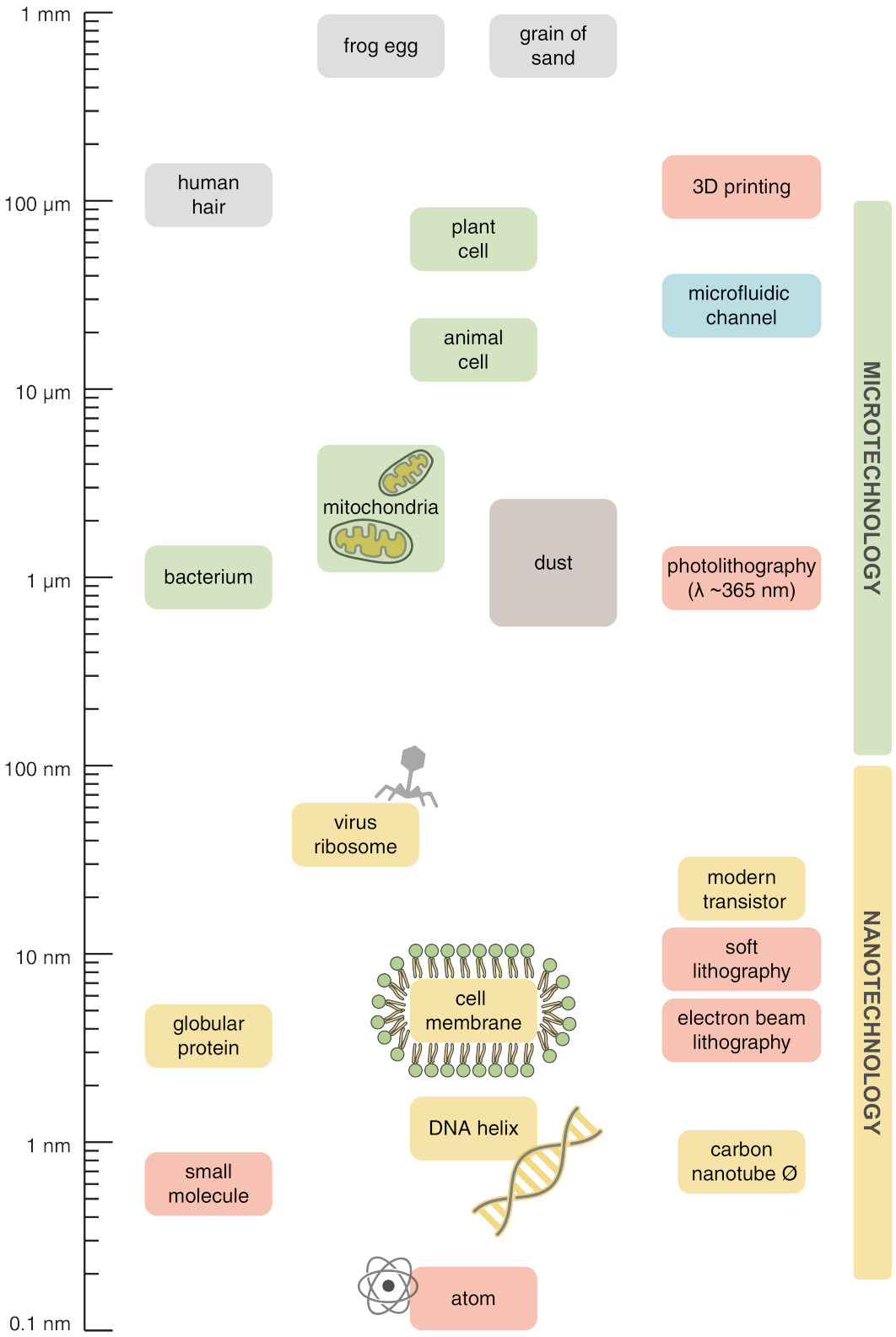

Figure 1.1: Biological and technological size scales, including sizes of various entities and experimental resolution limits.

Chapter 2. Biological Cells and Vesicles

2 Biological Cells and Vesicles

Discovered by Robert Hooke and named after a small room (Latin *cella*) in 1665, the biological cell is the fundamental structural and functional unit of living matter [2]. Millions of chemical reactions occur simultaneously in the interconnected system of organelles and the cytosol of a cell. Among other aspects, the research field of cell biology is directed towards a deeper understanding of this complex compartment in terms of its structure and mechanics [3, 4], components [5–7], metabolism [8–10], communication [11–13], development [12, 14, 15] and death [10, 16, 17].

In a multicellular organism, such as the human body, cells are differentiated into various types with specific and distinct functions. In mammals, the major cell types are skin cells, blood cells, neurons, muscle cells, fibroblasts, stem cells, and others in highly developed organs. Different cell types have different structures and functions. All cells are surrounded by a cell membrane, enclosing their intracellular structure and composition, establishing their identity, and separating their interior from the extracellular environment. This cell membrane constitutes a functional unit of the cell, where many proteins that mediate cell-to-cell communications, are incorporated. Protein-based communication is conducted either electrically or chemically, for example, via ion-channels and g-protein coupled receptors. In a multicellular organism, this cell communication is involved in complicated higher functions, for instance, operation of the immune system is conducted by the signaling between different immune cells. Thus, studying cells, especially in the context of cellular networks, can provide valuable information for understanding the function of tissues and the mechanisms of diseases.

Currently, most cell experiments are performed on a collective to obtain statistical data. However, recent research implies that cells of the same type and in the same local environment can differ dramatically [18]. Moreover, new evidence suggests that these differences in individual cells can influence the development, health and function of the entire cell population [19, 20]. For this reason, a new research area has emerged, which targets the heterogeneity of single cells, to provide a more complete picture of the cellular processes relevant

to healthy and pathological states. The progress of this field is, however, limited by the available techniques and methods for tracking, isolating, manipulating and analyzing single cells in adherent cell cultures and tissues. Consequently, the work described in this thesis focuses on the development of platforms and technologies for studying individual cells in controlled model environments.

2.1 Cellular Communication

In multicellular communities, groups or networks of individual cells perform specialized functions. In order to work efficiently, the cells communicate with each other in various forms. The main forms of cellular communication are:

1. paracrine [21] - signals are released into the extracellular space and act locally on neighboring cells,
2. endocrine [2] - hormones are secreted into the bloodstream for distribution,
3. contact-dependent [22] - through membrane-bound signal molecules and receptors, and
4. synaptic signalling [2] - neurons transmit signals electrically and release neurotransmitters at the synapses.

Cells rely heavily on communication to coordinate processes, which is necessary for the development of higher functions. Disruption in cellular communication can interfere with maintenance of homeostasis, function and reproduction, and may lead to severe pathological conditions in organisms, for example, the development of cancer [23]. Thus, it is important to develop a thorough fundamental understanding of cellular communication and its influence on the health of cell communities. Cells communicate extensively with their microenvironment and in response to chemo-attractants, they can form protrusions, or extensions of the cell membrane.

2.1.1 Cell Protrusions

Different cell types generate various protrusive structures [2]. Some cells also extend protrusions in an exploratory manner in the absence of a direct attractant. The protrusive structures are generally filled with dense cores of filamentous actin, and can be characterized by the way the actin is organized by the actin-cross-linking proteins. Protrusions, known as filopodia, have been implicated in cell migration and connection [24], virus transport [25], gene delivery [26], and even in cancer cell motility [27]. Despite extensive studies, the biological

functions and the mechanisms of their assembly are still not fully understood, but one of the primary biological functions of filopodia is to reach out from the cell to sense and probe the environment in response to chemical or mechanical cues [28].

In 2004, a study on tunnelling nanotubes (TNTs) was reported [11], implicating tubular membrane interconnections in cell-to-cell communication in mammalian cells and generating a strong interest in studying intercellular communication in cell protrusions. In this context, the possibility of controllably generating natural networks of living cells is a promising experimental environment. In **Paper I**, we designed a platform, utilizing a cytophobic fluoropolymer for exploiting the growth and connectivity of filopodia-like cell protrusions in order to provide more insight into cell-to-cell communication.

2.2 Cell Viability

Cell-based assays are often used to investigate the influence of compounds of interest on cell proliferation and function, in terms of detrimental effects and cytotoxicity that can eventually lead to cell death. In most basic viability assays, the term ”viability” could simply mean that the cells are not dead. For advanced cell studies, viability is explained in terms of proliferation [29], particular cellular functions, apoptosis (programmed cell death) or necrosis (cell injury which leads to premature cell death). Evaluation of cell proliferation requires following the development of cells for at least two generations, and includes incubation and careful monitoring. For this reason, major criteria employed for rapid cell viability are often based on the assessment of functionality [30], integrity of the cell membrane [31] and/or metabolic activity [32].

2.2.1 Viability Assays

One of the earliest cell viability assays is based on the compound Trypan Blue (TB), which probes the integrity of the cell plasma membrane [33]. The toluidine derivative is a hydrophilic compound, which means that it cannot be taken up by healthy cells. However, when the plasma membrane is injured, TB can cross the compromised cell membrane and accumulate in the cytoplasm, giving the characteristic blue color. Another common viability assay relies on the molecule Resazurin. The dye is weakly fluorescent, until it is reduced within the cytoplasm, making it a useful agent for measuring aerobic respiration. A carbocyanine nucleic acid stain, YO-PRO-1, can be used to identify apoptotic cells as they are permeant to YO-PRO-1, but remain impermeant to dead cell stains [34].

Fluorescein diacetate (FDA) is a cell-permeant, non-fluorescent derivative of fluorescein. FDA characterizes both cell membrane integrity and the activity of intracellular non-specific esterase enzymes. Once FDA has crossed the cell plasma membrane, the enzymes hydrolyze FDA into the fluorescent product fluorescein, which accumulates in the cytoplasm if the membrane is intact [35].

Propidium iodide (PI) is an intercalating agent and upon binding to nucleic acids becomes highly fluorescent. The internalization of (PI) by biological cells follows the same basic principle of Trypan Blue. PI molecules are membrane impermeant and are thus excluded from viable cells. Once the cell membrane is compromised, the molecules are free to enter and accumulate in the cytoplasm. PI can also be used to quantitatively assess DNA content [36].

Following an increase in dedicated experimental setups that can address cell heterogeneity, there is now a need to directly assay the viability of selected cells, without adversely affecting the majority of the surrounding cells. In **Paper II**, we present a rapid method for confined viability characterization of individual adherent single cells using propidium iodide (PI) and fluorescein diacetate (FDA). The two viability agents are commonly used in conjunction with one another [37], to characterize both cell membrane integrity and intracellular non-specific esterase enzyme activity.

2.3 Biological and Artificial Membranes

The plasma membrane of a cell encloses its intracellular structure and composition, and maintains the essential differences between the cytosol and the extracellular environment. It is composed of lipid molecules and proteins, where the lipids are arranged as a continuous, two-dimensional fluid bilayer of about 5 nm thickness, acting as a relatively impermeable barrier to most water-soluble molecules. Membrane proteins are arranged within this dynamic and fluid structure, where they mediate other functions of the membrane, such as signalling and transport of specific molecules.

Phospholipids are the most abundant molecules in the plasma membrane of biological cells, responsible for the structure and the flexibility. Their ability to form membranes stems from their amphiphilic character, meaning that they contain both a hydrophilic, polar end and a hydrophobic, non-polar end. Figure 2.1 illustrates the various types of amphiphilic molecules and their shapes. The spontaneously formed configurations are more energetically

favorable, and the geometry of these structures is dependent on the shape of the molecule [38]. Phospholipids are double-chain amphiphiles which spontaneously assemble into bilayers and vesicles in aqueous environments.

This spontaneous self-assembly can be exploited to generate artificial structures. For example, large artificial lipid vesicles, known as giant liposomes, are useful for studying certain properties of biological cells [39]. By reducing the structural complexity of the system, the hollow membrane constructs can serve as simple artificial cell models, where the focus may, for example, be on the membrane dynamics or transport properties. Small liposomes are also highly interesting for drug delivery applications in pharmaceutical research, and in cosmetic formulations [40].

Other classes of amphiphilic molecules, namely surfactants, have found a wide range of technical applications. For example, anionics are commonly used in soap and detergent formulations, and cationics are used as anticorrosion agents, flotation collectors and antistatic agents [41]. The use of vesicles based on non-ionic surfactants, known as *niosomes*, is starting to emerge. Niosomes, the surfactant-based equivalent of liposomes, are similarly classified according to their size, from around 20 nm to sub-100 μm.

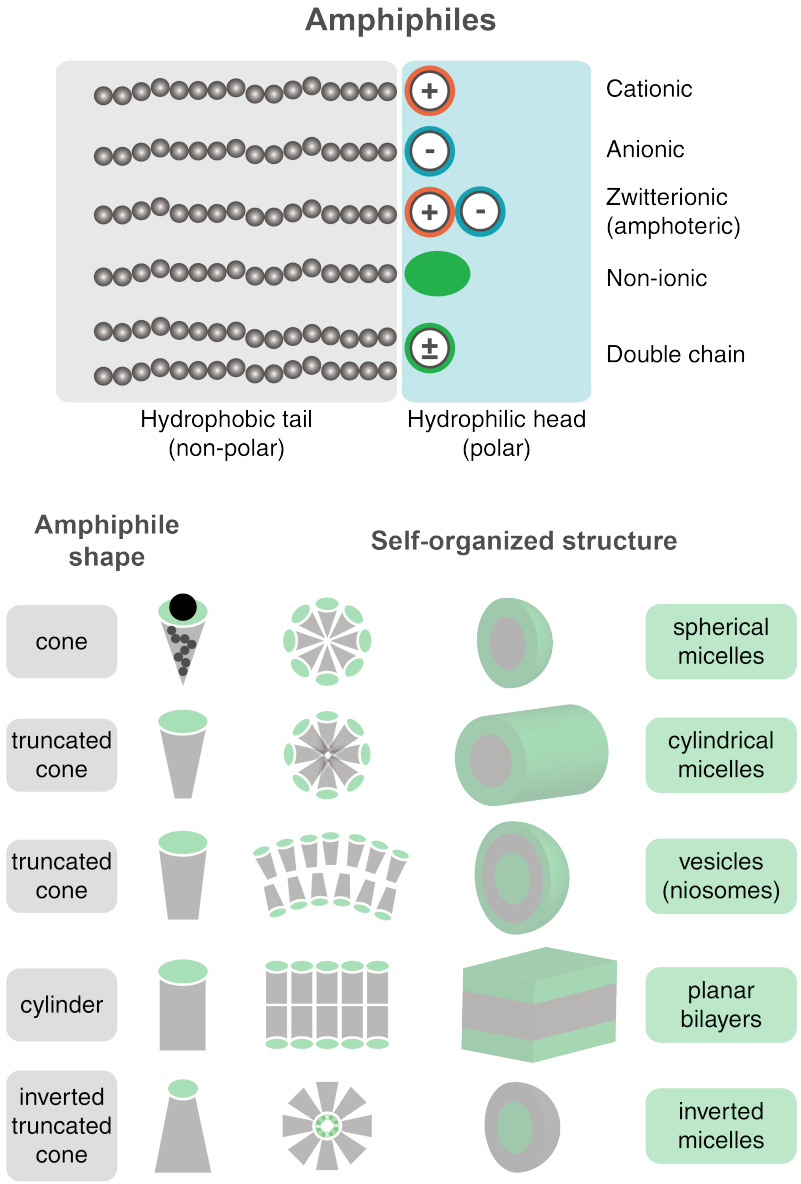

Figure 2.1: Schematic illustration of the various types of amphiphilic molecules, their shapes and their preferred aggregation structures in an aqueous environment. The grey color represents the hydrophobic, non-polar part and the green color represents the hydrophilic, polar part of the molecule. The double-chain amphiphiles can exist as non-ionic, cationic, anionic or zwitterionic molecules, indicated by the '±' sign.

2.3.1 Non-ionic Surfactants

Non-ionic surfactants are the second largest surfactant class, normally compatible with all other types of surfactants [41]. Contrary to ionic surfactants, the physicochemical properties of non-ionic surfactants are not greatly affected by electrolytes and they tend to maintain a near physiological pH in solution. They are particularly useful for stabilizing water-oil emulsions, but also find use as wetting agents, emulsifiers and permeability enhancers [41, 42]. Within vesicle preparations, they are preferred for their stability, biocompatibility and limited toxicity, in comparison to their ionic and amphoteric counterparts [42, 43].

Niosomes are a type of vesicle, self-assembled from non-ionic surfactants (neutral amphiphilic molecules) and cholesterol. They have become increasingly popular in pharmaceutical research, most notably for their ability to deliver compounds across the blood-brain barrier [44]. In comparison to liposomes, niosomes have higher chemical stability, shelf-life and lower costs [42, 45]. Niosomes are capable of carrying both hydrophilic and hydrophobic compounds (see Figure 2.2). Hydrophilic compounds can either be entrapped in the aqueous compartment or adsorbed to the surface, and hydrophobic compounds can be integrated into the lipophilic domain of the bilayers [46].

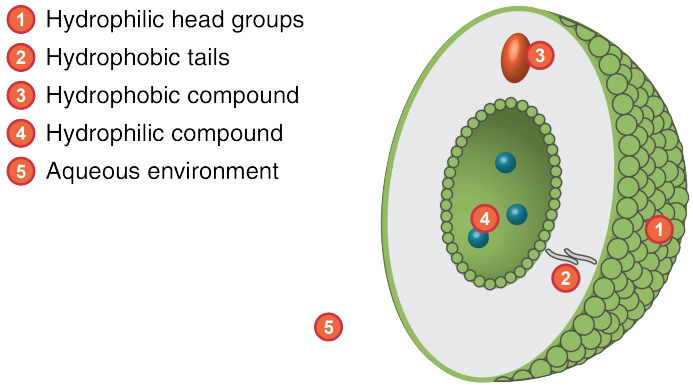

Figure 2.2: Schematic drawing of a niosome, illustrating the hydrophilic and hydrophobic parts of the vesicle. The green and the grey colors represent the hydrophilic and the hydrophobic parts, respectively. Two of the hydrophobic tails are outlined.

In the context of pharmaceutical research, niosomes hold promise as vehicles for drug delivery. Despite their potential, it is important to keep in mind that similarly to liposomes, they also have a risk of aggregation, drug leakage and/or hydrolysis of entrapped drugs during storage. Elucidating the molecular mechanisms that govern the interactions between niosomes and biological cells, and their uptake properties and retention, are necessary for successful

development of these artificial vesicle systems.

Current studies on biological and artificial membrane systems rely heavily on the use of fluorescent tags, which can influence the system under investigation. For this reason, we explored the possibility of using dielectric spectroscopy as an alternative label-free detection scheme, and we established a sensing platform in an open-volume fluidic configuration. Originally, the platform was developed for qualitative investigations of cholesterol content in model membranes [47]. In **Paper IV**, the work was extended for the characterization of two, structurally similar non-ionic surfactants.

Chapter 3. Microfabrication

3 Microfabrication

Prototyping of micro-scale platforms relies on microfabrication - a class of processing technologies that deals with fabrication of structures with at least one of the dimensions being in the micrometer range. It can generally be divided into two categories of top-down and bottom-up approaches. The bottom-up methods fall into the category of nanochemistry, using the chemical and physical properties of molecules in order to assemble different structures, and include strategies such as self-assembly and template chemistry [48]. Top-down techniques involve surface and bulk micro-machining, *i.e.*, methods that shape materials into microstructures, and include approaches such as laser ablation and photolithography.

This chapter presents an overview of commonly employed micro-processing techniques, with the focus on those used in this work.

3.1 Photolithography

Photolithography is a top-down approach for pattern transfer. It is the most commonly used technique due to its relative simplicity and sub-micrometer spatial resolution. The photolithography process generally consists of the following steps, illustrated in Figure 3.1.

1. Wafer cleaning
2. Resist deposition
3. Soft bake
4. Exposure
5. Development

Photolithography has extensively been used in this work, for prototyping of masters (Section 3.2), defining Teflon AF structures (Section 3.5.1), fabrication and bonding of SU-8 (Section 4.1), and for patterning thin metallic films.

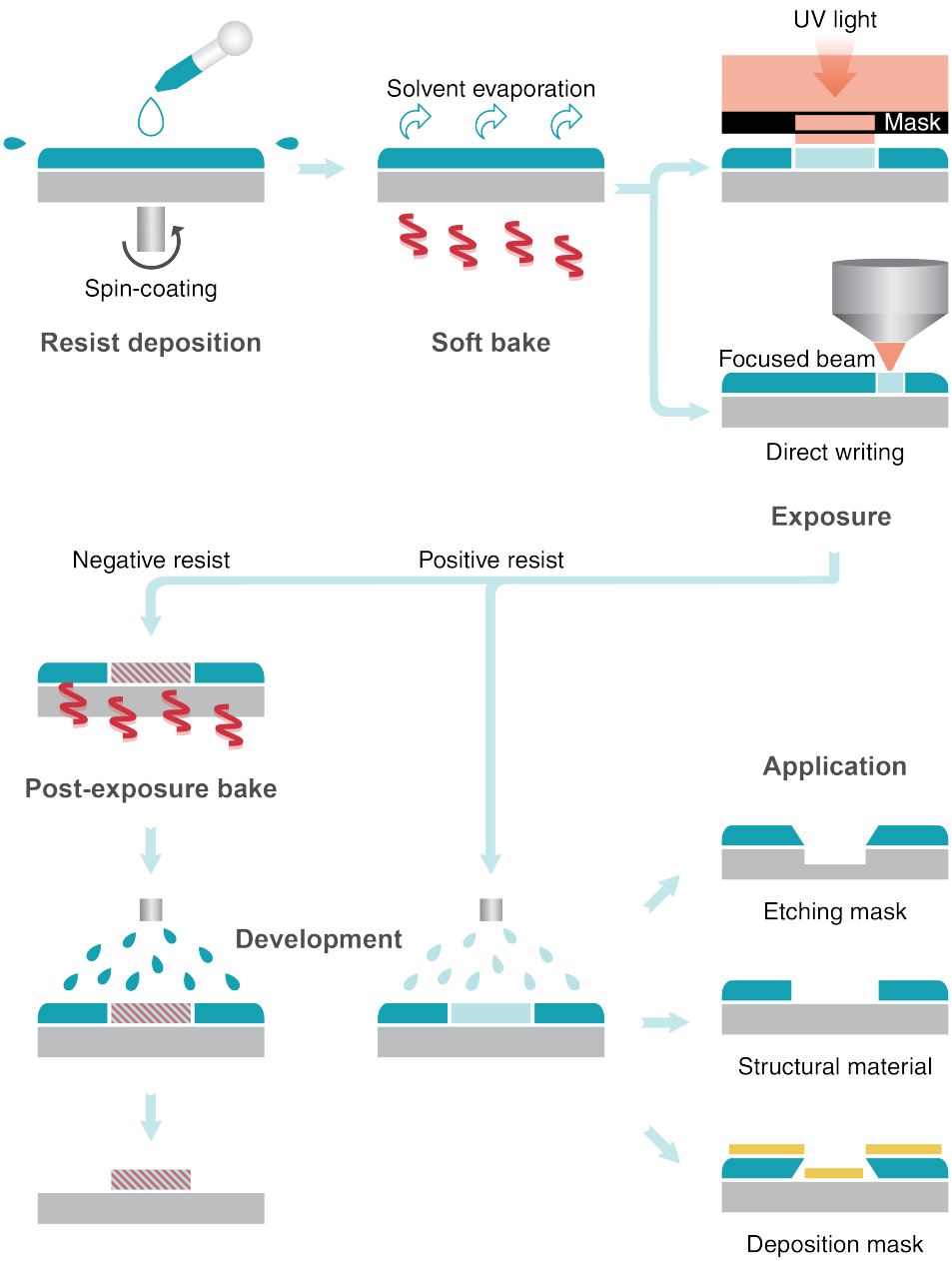

Figure 3.1: Photolithography. Examples of applications are illustrated with the positive tone resist. From top to bottom, the resist profiles are: overcut, vertical and undercut.

3.1.1 Photoresists

Photolithography utilizes UV light to induce changes in photosensitive materials, known as photoresists. The principal components of a photoresist are a polymer, a solvent and additives. Examples of additives include solubility modulating and photoactive compounds. The solvent and its evaporation rate control the viscosity of the resist formulation and the film quality. The photoresist changes its properties upon exposure to a light source by undergoing a chemical reaction, such as crosslinking, scission, change in polarity or change in reactivity. Photoresists are grouped into two categories: *positive* and *negative*. If a photoresist is of the negative tone, it means that the exposed parts of the polymer will be insoluble in the developing solution, in contrast to a positive photoresist.

The choice of the photoresist is influenced by its intended application, the processing method, and the pattern geometry. Generally speaking, negative resists have better adhesion to substrates and higher chemical resistance, whereas positive resists tend to have higher contrast and better thermal stability [49]. Due to illumination, differences in resist profiles occur as a consequence of backscattering and reflection effects, as photons collide with the surface at different angles. These differences are useful for different applications, for example, an undercut resist profile is advantageous for lift-off processes, whereas a vertical profile can be used to fabricate high precision structures (see Figure 3.1). Negative resists often result in either vertical or undercut profiles, and positive resists in overcut profiles, though multi-layered resist systems (lift-off layers) have been developed to produce undercut profiles.

3.1.2 Wafer Cleaning

Processing begins with thorough wafer cleaning to remove all contaminants from the surface of the substrate, such as solvent traces and particles. Different wet and dry methods exist for wafer cleaning, such as thermal treatment, plasma techniques, ultrasonic agitation and chemical processes, and their combinations.

Among the chemical processes used, RCA1 and RCA2 are the standard procedures, developed already in 1965 by Werner Kern. They are based on mixtures of hydrogen peroxide and various bases or acids, and are used to remove organic residues and metal ions, respectively. Ultrasonic and megasonic agitations, are mechanical methods, commonly used for removing micrometer- and sub-micrometer-sized particles from a surface. They are prone to contamination and can induce mechanical failure of deposited films.

Depending on the subsequent process, it may also be necessary to remove the native oxide of the substrate, which is commonly stripped by briefly dipping the wafer in a dilute aqueous solution of buffered hydrofluoric acid.

In addition to removing organic contamination, oxygen plasma treatment is commonly employed to modify the surface and thus change its adhesion properties. For this purpose, adhesion promoters can also be employed prior to photoresist deposition to improve the wetting properties of the substrate.

3.1.3 Resist Deposition

Common methods for photoresist deposition include spin-coating, spray coating, dip coating and casting methods with spin-coating being one of the most common methods in a laboratory setting. The photoresist is dispensed on a substrate, centered and held in place by a vacuum chuck on a motor. Typically, a low rotation speed ($\leq$ 500 rpm) is used to dispense the resist and cover the surface. After the dispensing step, the substrate is accelerated to a higher speed in the range between 1000 and 6000 rpm. The spin speed, duration and solvent properties, in particular the viscosity, will determine the final film thickness. The resist deposition step is critical as the photoresist film must have a uniform thickness for a homogeneous response to the subsequent exposure and development steps.

3.1.4 Soft Bake

During the soft bake, the resist film is heated to evaporate solvents, minimize stress and promote adhesion of the photoresist to the substrate. The resist thickness is reduced in this step. Excessive baking can destroy the photoactive compounds and decrease the sensitivity of the resist.

Typically, a hot plate or a convection oven is used for this step. For uniform heating, good contact between the hot plate and the substrate is required. If heating in a convection oven occurs too quickly, then solvent at the surface will evaporate first, forming a kind of resist skin and trapping the remaining solvent inside. Since the resist can reflow during the soft bake, for good quality films, this step needs to be performed on levelled surfaces for even planarization.

Lower initial bake temperature is recommended, as it allows the solvent to evaporate at a more controlled rate, resulting in a uniform coating and improved adhesion to the substrate. Ramp baking or step-wise heating are typically applied for sensitive resists.

3.1.5 Exposure

Following the soft bake, the resist-coated substrates are transferred to an exposure system. The purpose of the exposure system is to deliver light with the desired wavelength, intensity, directionality and uniformity across the substrate surface to produce a nearly identical transfer of the image onto the resist film. The wavelengths used in photolithography range from extreme ultraviolet (UV) to near UV. In near UV, the typical wavelengths used are g-line of 435 nm or i-line of 365 nm. After exposure, a post-exposure bake can be required so that the photochemical reactions initiated upon exposure to the light source can run to completion and modify the photoresist.

Photolithography commonly uses photomasks to transfer the pattern onto the resist film. Common materials for photomasks are soda lime glass, quartz, and polymeric films, all differing in resolution, wavelength-transparency, and cost. Soda lime glass and quartz are transparent to near UV light and deep UV, respectively. Mask-less photolithography is possible with direct writing by scanning a focused beam across the substrate coated with the photosensitive material. Direct writing is becoming more popular during research ande development, since the technique is more flexible. It does not require the fabrication of a photomask, and the resolution is comparable to conventional photolithography, however, direct writing is also more time-consuming.

3.1.6 Development

Development is the selective dissolution of the resist film, resulting in a structural representation of the exposure pattern on the substrate. There are two approaches for development - wet and dry, with wet development currently being pre-dominantly used. Dry development is generally based on a vapor phase process or a plasma [48]. Wet development is solvent-based and depends on three types of exposure-induced changes to the photoresist: variation in the molecular weight of the polymer, reactivity change and a change of polarity.

Organic solvents may lead to some swelling of the resist during development, leading to a loss of adhesion between the substrate and the resist film. Aqueous development is highly favored for cost and environmental reasons, but requires the addition of surfactants to ensure uniform wetting.

Post-development processes include descumming, which is a mild oxygen plasma treatment commonly used to remove resist residues. A post-baking step can also be performed

at the end in order to remove residual solvent, anneal the film to promote the adhesion of the resist and improve the mechanical properties of the resulting film. Compared to soft and post-exposure baking, post-baking generally occurs at higher temperatures and longer times.

3.2 Soft Lithography

Soft lithography is the collection of techniques, which use elastomeric, soft materials to transfer micro-scale patterns, for both into and onto a substrate [50–53].

By casting an elastomer in a master mold, in a process known as replica molding, microfluidic chips for prototyping can be fabricated. The master mold typically consists of a patterned silicon wafer, produced either by dry etching into the bulk of the surface or by photolithographic patterning of a photoresist (commonly SU-8, see Section 4.1). Structures larger than 100 μm can be milled in polymeric substrates. The surface of the silicon mold is chemically treated prior to casting in order to facilitate the removal of the silicone elastomer once it is cured. Figure 3.2 illustrates the fabrication process of microfluidic chips.

Currently, the widely favored material for soft lithography is polydimethylsiloxane (PDMS), further described in Section 4.3. The low interfacial free energy, chemical inertness, optical transparency and good thermal stability of the material make it a particularly suitable prototyping material for soft lithography [48].

Soft lithography is capable of fabricating structures from tens of nanometers to hundreds of micrometers [51, 54, 55]. The deformability of the elastomer allows it to make flexible devices and to accommodate non-planar surfaces. Short turn-around time, low cost and relatively simple equipment requirements make it an advantageous lithographic technique. Soft lithography has been used in a wide range of applications, such as direct fabrication of nano- and microfluidic devices [56, 57], and stamps for pattern transfer. In pattern transfer, applications include patterning proteins [58, 59] and cells [60], organic transistors [61, 62] and biosensors [63, 64].

3.3 Thin Film Deposition

A thin film is a layer of material, ranging from a nanometer to several micrometers in thickness on a substrate. Thin film deposition refers to a set of techniques, important in solid-state

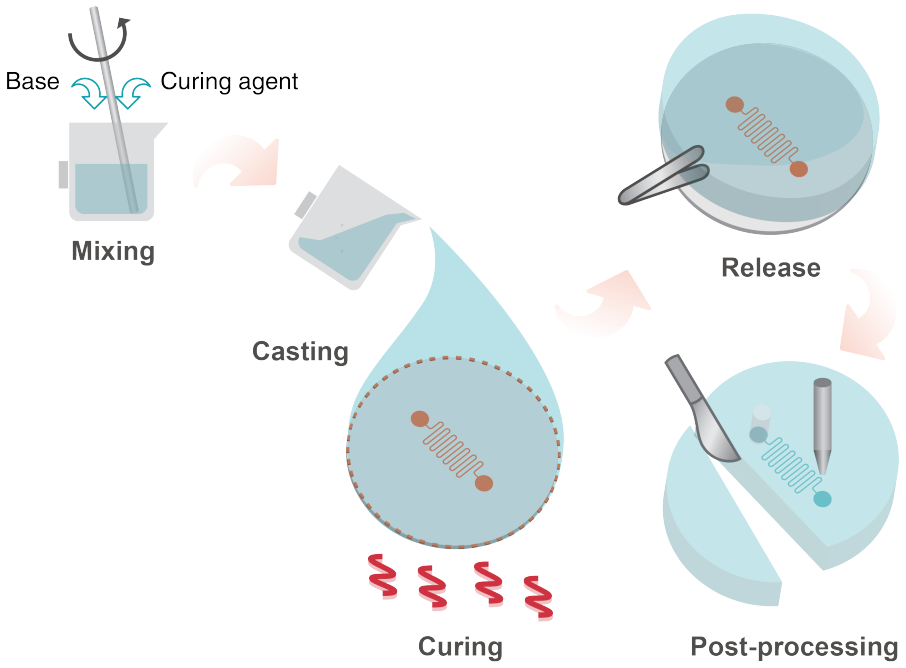

Figure 3.2: The process of replica molding. First, the two-component pre-polymer is mixed and degassed. Then it is poured onto a surface-passivated, patterned wafer, indicated by the dashed orange lines, and heat-cured. After curing the elastomer can easily be released. Post-processing can include punching of ports, bonding, and cutting to shape the material.

microfabrication. There is a number of deposition techniques available, depending on the material and the thickness of the thin film required. The deposition approach has a very profound effect on the resulting thin film, with differences in terms of density, crystalline orientation (if applicable), stress, roughness, surface energy, among others.

A number of additional thin-film deposition techniques exists, examples include electroplating, sol-gel, and spray- and spin-coating [48].

3.3.1 Physical Vapor Deposition

Physical vapor deposition (PVD) is a versatile technology for deposition of thin films. It can be used to deposit different kinds of materials: metals, alloys, ceramics, and polymers, on a variety of substrates. The general idea behind PVD is to remove material from a solid target and transfer it to the substrate under vacuum conditions.

PVD techniques can be grouped into the following five categories:

1. thermal evaporation
2. sputtering
3. ion plating and cluster deposition
4. aerosol deposition (ceramic coatings)
5. laser sputter deposition or laser ablation deposition (complex compounds)

Metallic thin films are most commonly deposited using sputtering and evaporation techniques. Sputtering has good step coverage and adhesion to the substrate and can be used for metals, alloys, ceramics and polymers. Reactive gases can be used to deposit films of chemical compounds, that are formed by reaction of the gas and the sputtered metal. Thermal evaporation is used mainly to deposit pure metals, and the technique works by transforming the target material from solid to vapor state and then letting the material condense onto the substrate surface. In comparison to sputtering, the step coverage is less, *i.e.*, the side walls are not covered with the deposited material. This can be advantageous, for example, in the case of patterning metallic layers by sacrificial etching of the material underneath, in a process known as lift-off (see Section 3.5.1).

Evaporation and sputtering were extensively used in the work presented in this thesis. Thermal evaporation was primarily used for directional deposition of metallic films, in order to facilitate subsequent processing, and sputtering for reactive deposition of oxides and nitrides.

3.3.2 Chemical Vapor Deposition

Chemical vapor deposition (CVD) is a broad class of processes that uses controlled chemical reactions to create thin films on substrates. The material precursors in the vapor phase often diluted with an inert gas carrier, adsorb on a hot (above 300 °C) surface of a substrate and undergo a chemical transformation, forming a thin film. In plasma-enhanced CVD (PECVD), homogeneous gas phase reactions are initiated using a plasma generated by a radio-frequency source instead of thermal energy, allowing for the process to be carried out at a much lower temperature [48]. Atomic layer deposition (ALD) is considered a subclass of chemical vapor deposition techniques. It employs sequential deposition of individual monolayers at the surface in a highly controlled manner, resulting in atomic scale precision.

In this thesis, CVD was used for deposition of oxide films as a passivation layer in the fabrication of millimeter-wave devices.

3.4 Bonding

In microfabrication, bonding refers to a collection of techniques for reversible or irreversibly adhering substrate surfaces. Micromechanical and nanomechanical systems (MEMS and NEMS) can require bonding techniques for component integration, and to ensure mechanically stable and sealed environments to protect sensitive internal structures from surrounding influences, such as temperature, high pressure, and moisture. Bonding is also an important technique in microfluidic systems, allowing the formation of cavities and sealed channels.

Bonding can be separated into two categories - (1) direct and (2) indirect bonding. Indirect bonding operates by means of an intermediate layer and direct bonding relies on strong chemical bonds between two substrate surfaces.

3.4.1 Direct Bonding

Direct bonding usually involves two identical or similar materials, for example, silicon–silicon or silicon–glass. The process of bonding one silicon wafer to another is known as silicon fusion bonding, and it is based on the chemical reaction between the native oxide layers. Two wafers, in very close contact, are heated in an oxidizing environment to extremely high temperatures above 800 °C, but below the melting point of silicon of 1410 °C. Silicon can bond to glass in field-assisted thermal bonding, also known as anodic bonding [65]. The applied voltage, between 200 and 1000 V, creates a strong electrostatic field that pulls the substrates together. At high temperature, between 300 and 500 °C, the oxygen ions move towards the interface where they can react with silicon and form strong Si–O covalent bonds [49, 65].

Polymers, such as PDMS and SU-8 can also be bonded directly. PDMS can bond either to itself or to glass, through a plasma-activated condensation reaction, where the silicon–oxygen bonding allows the formation of covalent bonds between the two substrates. In the case of SU-8, the presence of unreacted surface sites (dangling bonds) allows two substrates to undergo polymerization to form a stable bond. This can be induced at relatively low temperatures and moderate pressure. Increasing the number of dangling bonds can be achieved by minimizing the degree of the crosslinking density of the photoresist [66] at prior processing steps and/or by exposure to 254 nm UV light [67].

3.4.2 Indirect Bonding

Adhesive bonding is an example of indirect bonding, where a polymeric material is used as an intermediate layer. The main advantages of this method are low processing temperatures (commonly below 200 °C), tolerance to particle contamination and bonding of patterned layers [65]. The disadvantages of adhesive bonding include limited long-term stability and thermal range, and poor mechanical properties [49, 65]. UV adhesives such as SU-8 require transparent substrates, but can be activated at relatively low temperatures.

In processes that rely on elevated temperatures, the coefficients of thermal expansion of the two different materials have to be taken into consideration to avoid micro-cracking and to ensure a well-defined contact area. This applies to all bonding techniques that involve different materials and high temperature processing.

3.5 Sacrificial Layers

Sacrificial layers in photolithographic processes allow the fabrication of partially attached microstructures and free-standing devices. The ability to implement such features enables the assembly of a wide range of devices, from cantilevers [55] to single-cell grippers [68], and the protection of structures during microfabrication [69]. Common sacrificial materials include silicon [70], oxides [71], metals [72, 73], and photoresists [74, 75]. The choice of the sacrificial layer is often connected to the practical implementation in the process. For example, if silicon dioxide is used as the sacrificial material, then its removal can require HF-based etching, which would limit the direct use of metals in the device to gold, nickel and molybdenum [65].

In the case of SU-8 (see Section 4.1), the production of free-standing devices is limited by the ability to lift-off structures in high yield. In **Paper III**, we introduce a novel sacrificial layer, thermal release tape, enabling an entirely mechanical release of the final devices.

3.5.1 Lift-off

Lift-off process is a microstructuring method, which uses a sacrificial material (typically a photoresist) for creating patterns. Figure 3.3 shows a typical lift-off process, illustrated for

micropatterning of Teflon AF and evaporated metal films. Lift-off was used in **Paper I**, to create guiding structures with specific surface topography that enabled investigations of cellular protrusions in free-space. This was achieved by photoresist swelling underneath the Teflon AF film, which lead to breaking and lift-off at the edges of the structures.

Lift-off was also used in **Paper IV** for defining metallic patterns. In this case, the metal film was evaporated to achieve directional deposition and ensure high-resolution structures.

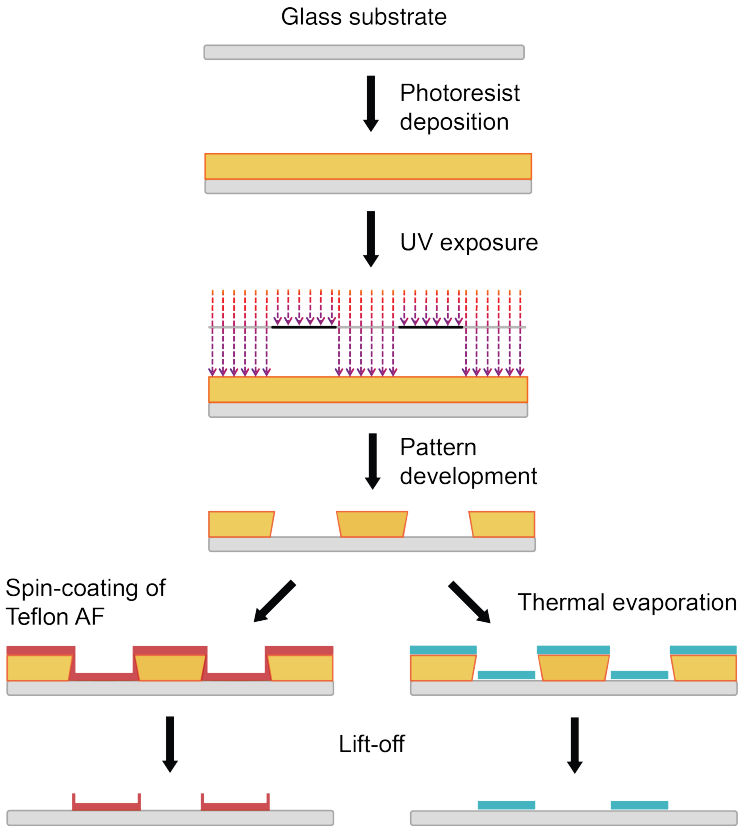

Figure 3.3: The lift-off process, illustrated for spin-coated Teflon AF and a thermally evaporated thin film.

Sacrificial etching is preferably the last step in the microfabrication process to avoid damaging the partially-detached structures in further processing steps. For entirely free-standing microstructures, the sacrificial layer has to provide sufficient adhesion and strength to the material of interest to avoid preliminary delamination from the support wafer and unwanted lift-off of the microstructures during the processing.

Chapter 4. Materials

4 Materials

Device performance and fabrication options depend, to a large extent, on the choice of the material. Considerations include device requirements, process parameters, device integration and intended applications. Microsystems for biological and biomedical applications commonly employ silicon, glass, thermoplastics, thermoplastic elastomers and biopolymers in device fabrication. In my work, the important engineering materials were Teflon AF, SU-8 and PDMS, with glass and silicon acting mainly as substrates.

4.1 Teflon® AF

Poly-(4,5-difluoro-2,2-bis(trifluoromethyl)-1,3-dioxole-co-tetrafluoroethylene) is a well-known polytetrafluoroethylene (PTFE)-based compound, under the trade name Teflon amorphous fluoropolymer (AF). Teflon AF has great thermal stability, chemical inertness and low surface energy. It has excellent optical transparency and low autofluorescence, and its thin films allow for high gas permeability [76]; properties which make it a suitable material choice for many applications. Currently, it is most commonly used as a protective coating layer [77, 78], and as an insulator in electronics [79].

Teflon AF is a cleanroom-compatible material. However, since it is not a resist nano- and micropatterning of the material has been challenging. Some of the current techniques for patterning this class of materials include etching by means of a focused ion beam (FIB) [80], synchrotron radiation [81, 82], thermo-molding [83], and electron beam patterning [84] and irradiation [85]. Electron beam irradiation changes the solubility of Teflon AF in perfluorinated solvents. Photolithographic methods for patterning Teflon AF surfaces have also been reported, with features in the range of micrometers [86, 87].

Biological studies with Teflon AF have shown that the material is highly biocompatible [88], and it was used for investigations as a substrate in biological membrane studies [85, 86] and cell patterning [89]. The material was particularly suitable for our studies in **Paper I**,

for its ability to guide cell growth based on its cytophobic but not cytotoxic properties [87]. We employed a photolithography-based process for patterning micrometer-size features on glass substrates, ensuring a specific surface topography which enabled the growth of cellular protrusions in free-space.

Thermal bonding of Teflon plastics has also been reported [83, 90], enabling microfabrication of microfluidic chips based entirely in the perfluorinated polymers. These devices have found use in areas ranging from cell culture growth to petrochemical applications [83, 91, 92].

4.2 SU-8

Originally developed in the late 1980s, SU-8 is an epoxy-based negative photoresist. A single SU-8 oligomer contains on average eight epoxy groups. SU-8 is chemically inert, thermally stable, features high resolution and high aspect ratio, making it an ideal candidate for permanent MEMS structures. SU-8 is an amplified resist, which means that it contains a photo-acid generator (PAG). The photoacid is released during exposure and crosslinks the oligomeric epoxy during the subsequent post-exposure bake step, resulting in a three-dimensional network. Figure 4.1 illustrates the chemistry of the SU-8 resist during a photolithographic process.

4.2.1 Formulations

Since the original SU-8 series, two new formulations of SU-8 have been developed by MicroChem: the 2000 series and the 3000 series. The SU-8 2000 series can be used to create films in the range of 0.5 to 200 μm. The series offers improved wetting properties and high aspect ratios (above 10:1). The SU-8 3000 series is designed to produce films between 5 and 120 μm. The aspect ratio is lower (above 5:1), but the series offer improved adhesion to oxides and nitrides [93]. The company, DJ DevCorp, is developing thick dry film sheets, and they are offering SUEX, an almost solvent-free formulation of SU-8. The photoresist sheets are in the thickness range of 100 μm to 1 mm and can be directly laminated onto substrates, offering a high process speed and thickness uniformity.

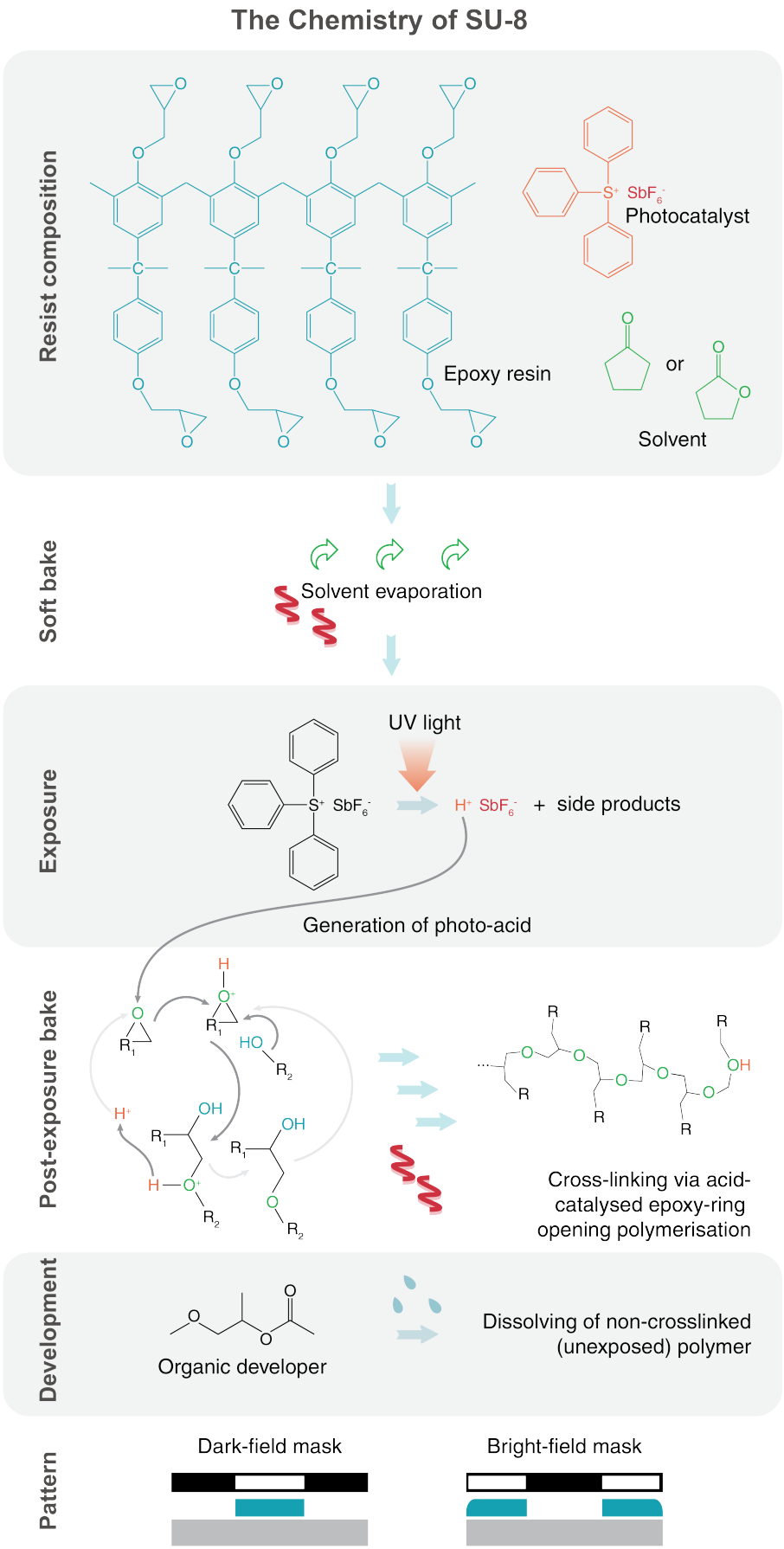

Figure 4.1: The chemistry of SU-8, a negative tone epoxy photoresist.

4.2.2 Multi-layer Photolithography

The initial amount of solvent in the resist formulation controls the available film thicknesses. Purposefully retaining solvent in SU-8 films has been used for fabrication of solvent-controlled nano-porous structures [94]. Otherwise, a soft bake is typically performed after initial film deposition to remove excess solvent and to improve adhesion to the substrate. This determines the residual solvent concentration in the SU-8 resist at the time of exposure, and the onset of crosslinking. Low solvent content also reduces the diffusion of the photo-acid and limits the mobility of the oligomers in the polymer matrix. This step leads to some shrinkage and stress in the film. It has been shown that thinner films exhibit higher film stress [95], which can lead to formation of fractures in the material.

The volatility of the solvent in SU-8 formulations leads to a decrease of the solvent content already at ambient temperatures [94, 96]. For this reason, modern spin-coating systems are constructed to minimize solvent evaporation rate and air turbulence inside the spin chamber. Such systems allow the production of reasonably flat films without edge defects. For removal of edge beads, it is common to spray the periphery of the wafer with a solvent, after the soft bake. Even though SU-8 is designed to obtain planar films, planarization defects can still occur when working with resist formulations of high viscosities. SU-8 tends to follow the morphology of the substrate it is applied on. Leaving the resist to relax on a very flat-levelled surface after spin-coating promotes planarization, and can even reduce mechanical stress [97].

SU-8 polymerization can be initiated by UV light at 365 nm, but also electrons and ionizing radiation can initiate a high level of crosslinking [48]. During exposure, the photoinitiator generates a strong acid and catalyzes the cationic polymerization of the epoxy resin. The post-exposure bake is typically performed subsequently at 95 °C and then developed in an organic solvent. The final SU-8 devices can be hard baked further at 200 °C to complete the polymerization process, anneal the film, and minimize stress. Cured SU-8, after the post-exposure bake, has a glass transition temperature of above 200 °C, whereas unexposed SU-8 has a glass transition temperature of around 55 °C [98].

SU-8 resist can be patterned in the millimeter range thickness with aspect ratios up to 20 in a single photolithographic exposure [95, 99]. Ultra-high aspect ratios of 190 (6 μm thick and 1150 μm tall) have also been reported using wavelength optimization and air gap compensation [100]. Multi-layer structures can be obtained in SU-8 by successive processing of resist layers applied on top of each other. This is achieved by deposition, soft baking, exposure and post-exposure baking of every individual layer followed by simultaneous development [101].

4.2.3 Sacrificial Layers

Extensive research has been done to accomplish hanging structures and free-standing devices in SU-8, in order to exploit its favorable mechanical and chemical properties. To achieve this, metallic sacrificial layers such as aluminum [102] and copper [103] have been used in combination with wet etching. Other sacrificial layers include: oxides [104], the overhead projector (OHP) transparency film [105], Kapton (polyimide) film in combination with a positive photoresist [66, 106] and polyester [107] or Mylar [108] sheets, polystyrene [109] and even PDMS [110]. OmniCoat has also been used for this purpose [111, 112]. In **Paper III**, we utilized thermal release tape to achieve an entirely mechanical release of SU-8 devices.

4.2.4 Surface Chemistry

SU-8 has a hydrophobic character, with a contact angle of $79 \pm 1^\circ$ [113]. In order to improve the wetting characteristics of channel devices, there is a number of ways available for rendering an SU-8 surface more hydrophilic. Exposure to oxygen plasma is the most popular technique. The effect of oxygen plasma is a highly hydrophilic surface, with a small contact angle of $\sim 5^\circ$, directly after the treatment[114].

An alternative method involves a wet chemical process, in which the surface of SU-8 is exposed to ethanolamine, which leads to a contact angle of $23 \pm 7^\circ$ [115]. The SU-8 surfaces are modified by the reaction between the amino groups in ethanolamine and the remaining unreacted epoxy groups [115]. The resulting contact angle does not increase over time, in contrast to oxygen plasma treated surfaces.

The bulk of SU-8 can be permanently modified by the addition of a small organic molecule, glycidol, which contains both epoxy and hydrophilic functional groups. The resulting copolymer has a contact angle of around 55° [116], but suffers from an increase in fragility.

4.2.5 Bonding

SU-8 can be bonded directly to SU-8, if there are enough active sites present at the surface (unreacted epoxy groups). Then, two substrates can undergo a polymerization reaction to form a stable bond, at relatively low temperatures and moderate pressure. Increasing the number of dangling bonds, provided through unreacted epoxy groups, on the surface can be achieved by under-baking of the resist [66] and/or by exposure to 254 nm UV light [67]. SU-8 has been used for both direct, and adhesive bonding.

4.2.6 Challenges

Despite many of its useful characteristic properties, SU-8 has like all materials its limitations. Many of the standard SU-8 fabrication processes require hands-on experience and optimization. SU-8 is considered a chemically stable material, once it is crosslinked. However, exposure to certain solvents (such as acetone) can modify the surface or crack the structures. SU-8 has unfortunately high autofluorescence in comparison to, e.g., Teflon AF. This makes it a challenge to combine the material with fluorescence microscopy techniques, commonly employed in the life sciences.

SU-8 is, however, a suitable material choice in the development of label-free experimental setups. In addition, even though it is generally considered a biocompatible material [117], the base of SU-8 is Bisphenol A, a well-known endocrine disruptor [118]. This might be an issue in long-term biological studies that involve SU-8 devices.

SU-8 is a very popular material choice in MEMS and for master fabrication in soft lithography. In the life sciences, it has been used in a wide range of applications, both as support and main material. Some examples include microgrippers for single-cells [119], force sensing arrays [120], and microprobes [102, 108] for neural applications. The primary use of SU-8, in this thesis, has been for the establishment of a facile microfabrication process for the development of free-standing microfluidic probes, presented in **Paper III**.

4.3 Polydimethylsiloxane

Crosslinked polydimethylsiloxane (PDMS) is a silicone elastomer with many favorable properties. PDMS is gas permeable and chemically inert and it is generally considered non-toxic and biocompatible. The material is optically transparent (below 280 nm) with relatively low autofluorescence, making it a good candidate for microscopy-based studies. PDMS is often used in soft lithography as the stamp material due to its low cost, elasticity and low surface tension. Figure 4.2 illustrates the chemical structure of the siloxane oligomers and crosslinkers and the polymerization reaction that leads to the formation of the elastomer.

PDMS is generally prepared using a standard kit of two components, consisting of a ”base” (siloxane oligomers) and a ”curing agent” (siloxane crosslinkers and the catalyst), such as SYLGARD® 184 from DOW Corning. Other silicone variations are available from DOW

Corning for electronics (170) and with modified properties, such as flame resistance (160).

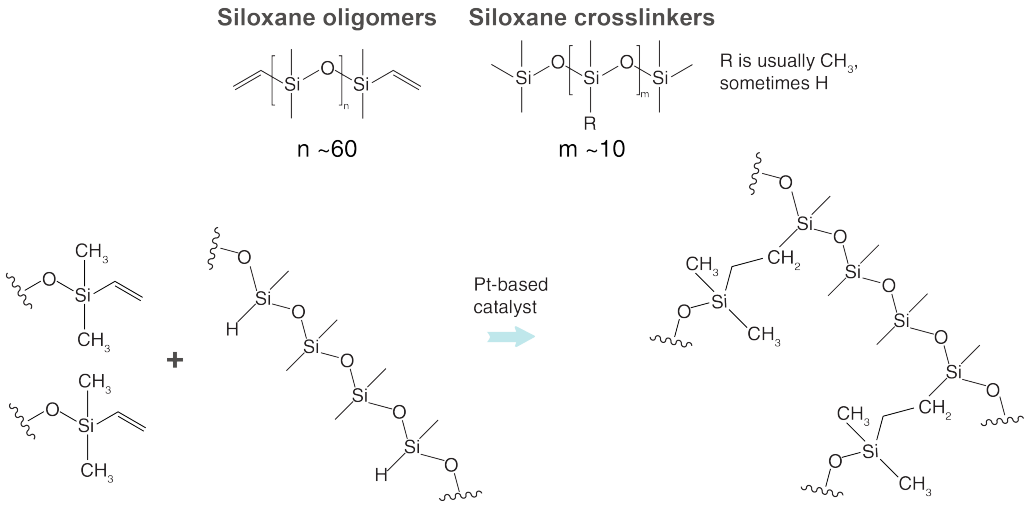

Figure 4.2: The chemical structure of the siloxane oligomers and crosslinkers, illustrating the chemical reaction that occurs during the formation of the three-dimensional polymer network.

The ”base” and the ”curing agent” are mixed in the recommended proportions (usually 10:1) to form, what is often referred to as the PDMS pre-polymer. This mixture is degassed to remove air bubbles and cured. The curing process is commonly performed between temperatures of 60 and 95 °C, with a Pt-based catalyst, for example, hexachloroplatinic acid. Thin PDMS layers in the range of a few micrometers can easily be achieved by spin-coating [121, 122], and films as thin as 70 nm have been reported by diluting PDMS with hexane [123].

The surface of PDMS can be modified by exposure to oxygen plasma to become hydrophilic, replacing the methyl groups with hydroxide groups as illustrated in Figure 4.3. The modified surface of PDMS has a contact angle of $\sim 5°$, which gradually returns to its hydrophobic state [124], as the silanol groups move into the bulk of the material to minimize the surface energy. This process occurs relatively quickly due to the elasticity of PDMS. The surface modification procedure can be exploited to bond PDMS either to itself, or to glass, through a plasma-activated condensation reaction illustrated in Figure 4.3 [125]. Clean surfaces and good contact (planar surfaces) are critical for achieving a good quality bond. PDMS can also form a self-adhesive bond by conforming due its softness. This bond is weak, withstands approximately 0.5 MPa of pressure before delaminating. As long the surfaces remain clean, it can be de-bonded and re-bonded [65].

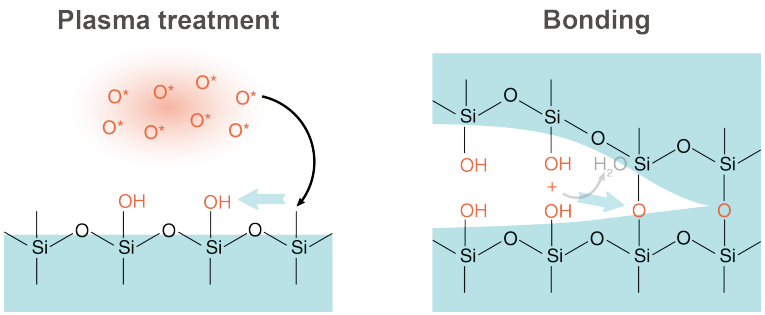

Figure 4.3: Plasma treatment and bonding of two PDMS surfaces.

From the manufacturing point-of-view, PDMS has a relatively long turn-around time, in comparison to materials that can be injection molded. The lack of compatibility with other materials creates a challenge in chip-to-world interface for high-pressure connections, where a conformal seal is not sufficient. Deposition of metal films on PDMS requires harsh conditions [126]. In addition, PDMS has low solvent compatibility [127], and it is not a commonly accepted material in cleanroom environments for reasons of contamination.

Despite some of its limitations, PDMS has found use in a wide range of applications. It has become a very important prototyping material in micro- [128, 129] and nanofluidics [130, 131], soft lithography [132, 133], traction force microscopy [134] and recently even soft robotics [135–137]. The superfusion device used in **Paper I** and **Paper II** for single-cell studies, has been manufactured in PDMS.

Chapter 5. Technology

5 Technology

Recent advancements in material science and microfabrication have significantly accelerated the development of miniaturized technologies, which consequently increased the research possibilities within the life sciences. The technological concepts presented in this chapter, focus on those relevant for this thesis, namely *Microfluidics* and *Electromagnetic Waves*.

5.1 Microfluidics

Microfluidic technologies are now commonly used in many research areas, such as diagnostics [138, 139], single-cell research [140, 141], cell culturing [142, 143], flow cytometry [144, 145], cell sorting [146, 147] and particle synthesis [148, 149], among many others. Microfluidics is the study of the behavior and the manipulation of small amounts of fluids, dealing with volumes in the femto- to microliter range. By exploiting the characteristics of fluids at those size scales, microfluidic technologies offer a number of advantages. In order to provide an insight into the technological benefits of microfluidics systems, this section introduces some of the physical characteristics present; beginning with the fluid motion at the micro-scale.

5.1.1 Fluid Motion

The Navier-Stokes equations describe the motion of fluid and are essential for understanding fluidic systems. The equations are derived using Newton's second law of motion. For an incompressible homogeneous Newtonian fluid the expression is

$$\rho\left(\frac{\partial \mathbf{v}}{\partial t} + \mathbf{v}\cdot\nabla\mathbf{v}\right) = \rho\mathbf{g} - \nabla P + \mu\nabla^2\mathbf{v} \tag{5.1}$$

where ρ denotes the density, $\mathbf{v}$ the flow velocity, ∇P the pressure gradient, μ the fluid viscosity and $\mathbf{g}$ the gravitational acceleration. The term on the left-hand side represents the forces of inertia, and the term $\mu\nabla^2\mathbf{v}$ represents the viscous forces.

The equation in its dimensionless form shows that it depends on one scaling parameter, known as the Reynolds number (*Re*)

$$Re = \frac{\rho v_0 L_0}{\mu} \tag{5.2}$$

where L_0 and v_0 are the characteristic size and velocity, dependent on channel geometry. *Re*, is the ratio of inertial to viscous forces. In the case $Re \gg 1$, inertia dominates, resulting in a turbulent flow. For low *Re* numbers $\ll 1$, the flow is considered laminar (see Figure 5.1).

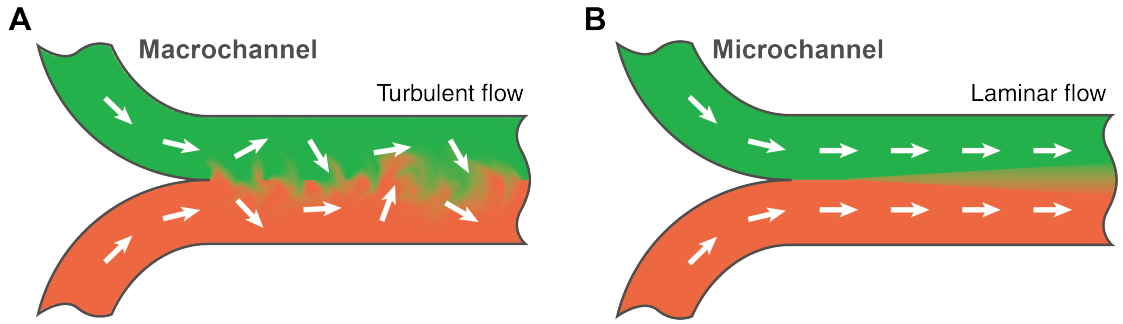

Figure 5.1: Fluid flow regimes. A) Turbulent and B) Laminar flows.

For microfluidic systems, the gravitational component is negligible and the fluid flow is considered free from fluctuations, as they typically operate at low *Re* values, in the laminar flow regime. Thus, the equation describing the fluid flow is simplified to the linear Stokes equation

$$\nabla P = \mu \nabla^2 \mathbf{v} \tag{5.3}$$

This equation can be solved analytically for a number of channel geometries by applying boundary conditions. Flow of liquid inside a microfluidic channel is typically subject to no-slip boundary conditions, meaning that the velocity field is zero at the wall and maximum at the center, giving a parabolic velocity profile. The resulting flow field can be integrated over the cross section of the channel to get an expression for the total flow rate [150]. The calculation of the flow rate is one of the most important parameters when it comes to the practical design and development of microfluidic chips.

5.1.2 Diffusion

Flowing solutions can co-exist in microfluidic channels under low *Re* conditions. Due to the lack of turbulence, spontaneous mixing does not occur, and diffusion is the only transport mode between the two parallel streams (see Figure 5.1B). Therefore microfluidic systems are

well-suited for fluid control and manipulation. They can be designed to handle a variety of solutions and reagents, mix and switch between flows, and carry out chemical reactions and bioassays on-chip.

For pure diffusion to occur, the velocity field of the fluid should be zero, otherwise the motion of the molecules within the fluid is also partly due to convection. In the regime of steady flows, the dimensionless Péclet number (*Pe*) is the relevant scaling parameter, describing the ratio between the convective and diffusive mass transports,

$$Pe = \frac{v_0 L_0}{D} \tag{5.4}$$

where D is the diffusion coefficient. A high *Pe* implies dominance of convection over diffusion, thus less diffusional mixing and sharper concentration gradients across the boundary of co-flowing streams. This concept is of particular importance for the operation of the hydrodynamic flow confinement (HFC) device, the multifunctional pipette (described below). In HFC devices, a high *Pe* is desirable to minimize the escape of molecular compounds via diffusion by using comparatively high flow rates.

5.1.3 Hydrodynamically Flow Confinement

Microfluidic technology is not limited to closed channels, which dominate in the traditional lab-on-a-chip view. Instead, a younger paradigm is emerging where the properties of micro-scale fluid flows are projected beyond the physical boundaries of a device into an open-volume. If the fluid emerges into the open volume, it can be re-captured, and led back into the device by sufficient neighboring in-flows. Proper channel geometry and distance, can allow such circulation to form a small reservoir, with virtual boundaries defined by the hydrodynamic flow (see Figure 5.2). The concentration gradient of the virtual boundaries is determined by the Péclet number, and the content of the reservoir is defined by the composition of the out-flow stream. This is known as hydrodynamic flow confinement (HFC) [151].

Initial HFC experimental setups for biological applications involved two glass capillaries, one for injection and one for aspiration (see Figure 5.2A). The HFC was approximately 30 μm in size, and the pressure switching allowed for local solution exchange, in the milli-second time scale [152]. The technique was used for stimulation of adherent neurons [152], potentiation of synapses [153], and studying motility of dendritic filopodia [154]. An improvement came with the co-axial pipettes, Picoliter 'fountain pen', which was the first free-standing HFC device [155] (see Figure 5.2B). In 2005, the Microfluidic Probe was reported as the

first microfabricated HFC device [156], which later evolved into the vertical Microfluidic Probe (vMP) [157]. The probe was used to pick up cells, pattern proteins, and stain adherent cells. Other relevant devices include the BioPen for direct writing of functional materials such as cells, proteins and nucleic acids for Point-of-Care diagnostics [158], the droplet-based chemistrode [159], and the push-pull probe for scanning electrochemical microscopy [160].

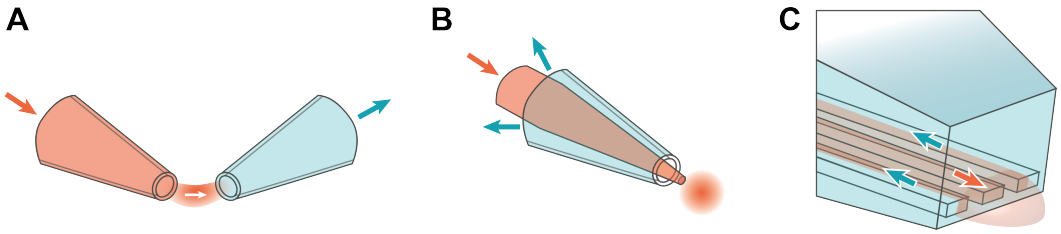

Figure 5.2: Schematic examples of HFC devices. A) Two glass pipettes, one for injection and one for aspiration [152]. B) Two co-axial glass pipettes, Picoliter 'fountain pen' [155]. C) Multifunctional Pipette (MFπ) in PDMS [161]. The arrows indicate the direction of the liquid flow. Orange color represents positive pressure and blue negative pressure.

The concept of hydrodynamic flow confinement has allowed the development of free-standing probes, which are easier to integrate with existing instrumentation and experimental environments, in particular in cell microscopy. The Multifunctional Pipette (MFπ) is an example of an HFC microfluidic device, refined for integration with other probes, upright microscopes and micromanipulators (see Figure 5.2C). The microfluidic device was developed for exchanging the solution environment (superfusion), and to provide local stimuli around single adherent cells.

In this thesis, MFπ was used to study molecular transport in cellular protrusions (**Paper I**) and viability of individual adherent cells (**Paper II**). In contrast to most HFC probes, which have two channels, this device has three adjacent micro-channels, which exit into an open volume. By adjusting the positive and the negative pressures in each channel, a semi-spherical HFC reservoir can be established. The generated isolated chemical environment at the tip of the device is typically 90 μm in diameter, with flow rates of 4-8 nL/s. The cells located within the HFC area experience little shear force, which does not affect cell viability [161]. Currently, MFπ is replica molded in PDMS; in **Paper III**, a novel microfabrication process was established for manufacturing the device in SU-8.

5.2 Electromagnetic Waves

Electromagnetic waves are simultaneous periodic variations of electric and magnetic fields that propagate from an emitting source at the speed of light when they are in vacuum. They are characterized by their wavelength or energy. Lower frequency corresponds to lower energy, with ionizing radiation (enough energy to completely remove an electron from an atom or a molecule) beginning at the end of the ultraviolet (UV) regime [162]. The spectrum of electromagnetic waves is illustrated in Figure 5.3.

Different regions of the electromagnetic spectrum have found different uses. For example, micro- and radio waves are mainly used for broadcasting and communication, and heating devices (e.g. microwave ovens). Moving higher on the frequency spectrum, the millimeter-wave scanner, a well-known device commonly used in airport security, is situated. Infrared spectroscopy is a widely used technique in organic and inorganic chemistry, for analysis of chemical compounds, and X-rays are essential in medical imaging (radiography) and high-energy physics.

The terahertz (THz) frequency regime is located between microwaves and far infrared. To a large extent it has remained unexplored, mainly due to lack of suitable instrumentation [163]. However, recent advancements in source and detector development have led to progress in applications of THz radiation in imaging [164, 165] and communication [166, 167]. The use of the THz frequency region in biomedical imaging and life science applications is just beginning to emerge. In biomedical research, applications such as imaging of cancerous tissues [168, 169] and *in vivo* imaging of burns [170] are being explored. In the life sciences, THz radiation has been used to investigate protein crystal interactions [171] and for spectroscopic analysis of biological molecules, such as proteins [172, 173] and RNA [174]. Currently, both opportunities and adverse effects of sub-millimeter-waves are being thoroughly investigated [175–177].

5.2.1 Dielectric Spectroscopy

Dielectric spectroscopy measures the dielectric properties of a medium as a function of frequency, and is based on the interactions between the external electric field with the electric dipole moment of the object of interest. This is commonly expressed as permittivity, which describes how an electric field affects and is affected by, a dielectric medium.

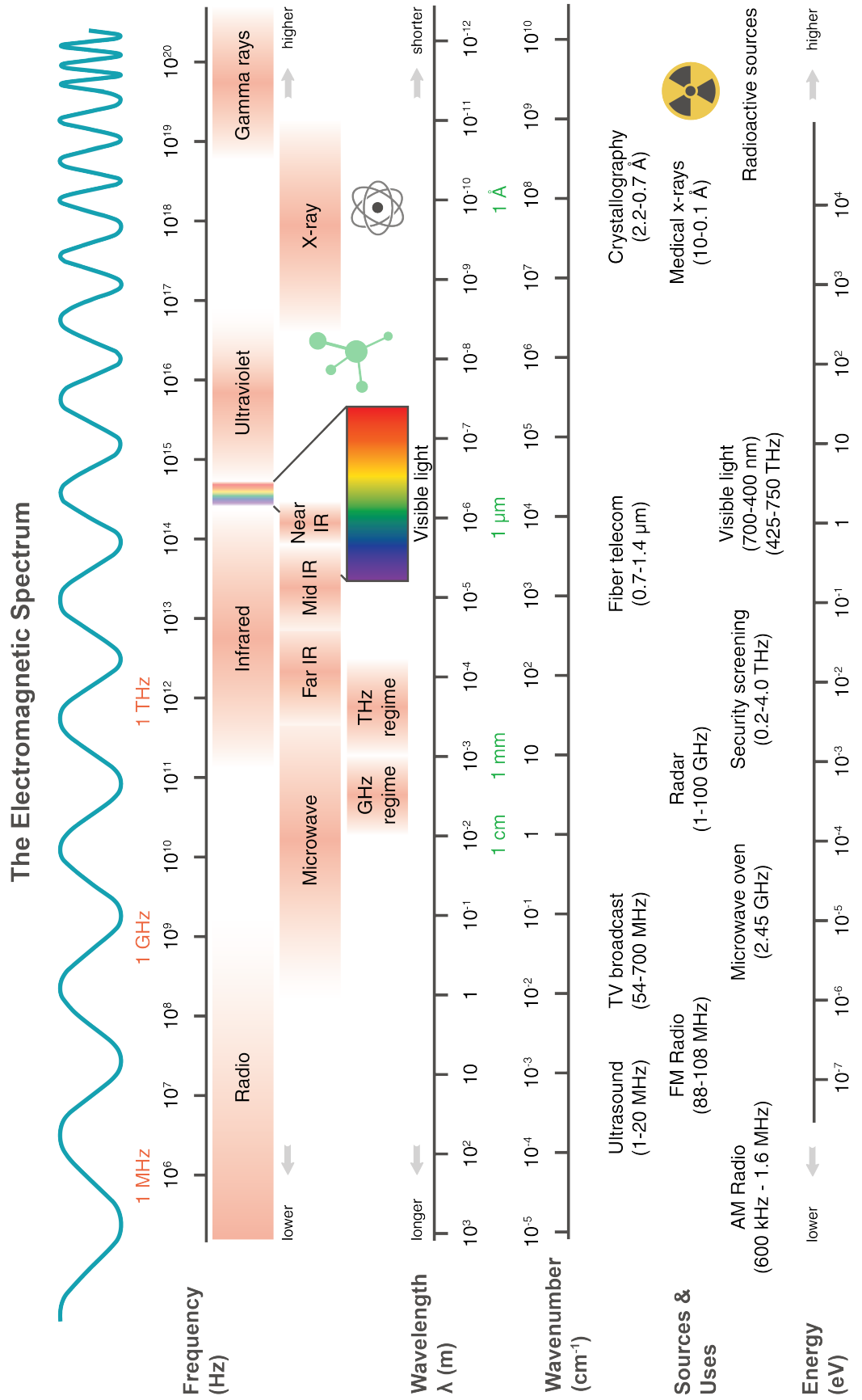

Figure 5.3: The electromagnetic spectrum

This spectroscopic method has become popular over the past few years, and is currently being employed to characterize coatings [178], films [179], solar cells [180], and surface corrosion [181], among others.

Dielectric spectroscopy is a non-invasive, label-free technique that can probe a sample in its native environment without the need for chemical modifications. In the life sciences, detection of binding events [182], membrane structure analysis [183], and studies of biological cells [184, 185], between the Hz and the MHz range have been reported.

Millimeter-Waves

The millimeter-wave (mm-wave) region, 30–300 GHz frequency band, has interesting implications in chemistry and life science research, as it contains information about molecular rotations, dielectric relaxations, and hydrogen bond interactions [186]. Currently, most of the research extends up to 40 GHz for label-free investigations on biological systems [187, 188], with recently reported work on yeast suspensions up to 110 GHz [189]. To fully scrutinize the significance of mm-waves in biological and biomedical applications, more information on the dielectric characteristics of biological entities is needed. In turn, this requires simple, affordable and versatile platforms, capable of investigating biological samples across the whole frequency band, which are not currently available.

In **Paper IV**, we present a flexible platform for dielectric spectroscopy on-wafer measurements of non-ionic surfactants, in the mm-wave region. We designed and fabricated microscale devices for propagating the electromagnetic waves, which allowed for the study of their interactions with our samples. The design is based on a coplanar waveguide (CPW), illustrated in Figure 5.4.

CPWs are commonly used for direct, on-wafer investigations of transmission and reflection of electromagnetic waves (amplitude and phase), as a function of frequency. It consists of a strip of thin metallic film deposited on the surface of a dielectric substrate, with two ground electrodes on each side and parallel to the strip, in a coplanar configuration [190].

The electric field lines of a CPW are illustrated in Figure 5.4. Changes in the material above the waveguide translate into changes of the effective permittivity of the CPW. As a consequence, the amplitude and the propagation velocity of the electromagnetic wave is modified. The effective permittivity of the CPW is given by the relationship between the permittivities of the substrate and the material above the sensor. We based the design of our devices on

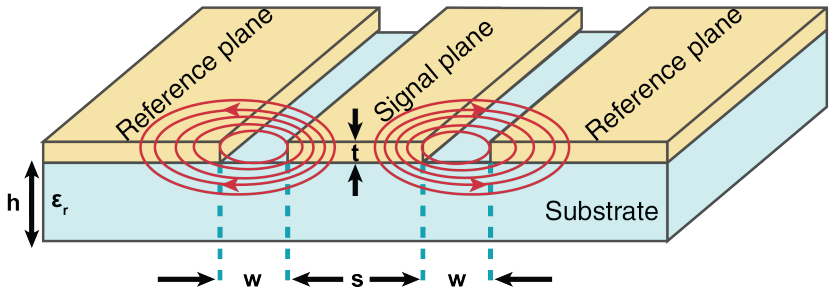

Figure 5.4: Schematic drawing of a coplanar waveguide. Critical dimensions, w (signal width) and s (signal-to-ground spacer) are indicated, and the red lines represent the electric field lines.

the CPW for its high surface sensitivity. Other waveguides, such as the microstrip [191, 192] and the Goubau line [193], are also being investigated for life science applications [194, 195].

The CPW-based devices were fabricated on glass substrates with polymer barriers for liquid confinement. For each molecular compound we investigated, several devices were measured separately by connecting them in turn to the measurement setup.

Our mm-wave setup consists of a vector network analyzer (VNA), a system that enables characterization of devices in terms of transmission and reflection of the electromagnetic wave (amplitude and phase), as a function of frequency. We used a two-port system, illustrated in Figure 5.5. The substrate with microdevices is placed on the stage and one of the devices is connected to the VNA via the radiofrequency (RF) probes. Standard RF probes are of the ground-signal-ground configuration, making them suitable for measurements of CPWs.

Prior to performing the measurements, a calibration involving known standards can be performed in order to compensate for systematic errors, and to set the reference plane at the probe tips. The test frequency is generated and its power level is set, typically in the μW range. The signal travels from one port to the other, and the transmitted and reflected powers are normalized to the input signal and recorded. The acquired results are expressed in terms of the scattering parameters (S-parameters), which can be described as the input vs. output relationship between ports in an electrical system. S_{21} represents the power transferred, as the signal travels to Port 2 from Port 1, following the naming convention of identifying the target port first. The signal travelling to Port 1 from Port 2 is denoted S_{12}. S_{11} and S_{22} are the respective reflection parameters. If the device circuitry is symmetric, the resulting parameters are identical, *i.e.*, S_{11} and S_{12} correspond to S_{22} and S_{21}, respectively.

Figure 5.5: Experimental setup. The inset illustrates two RF measurement probes connecting a single device to the vector network analyzer.

Building on our previous work [47], the platform presented in **Paper IV** is based on a coplanar waveguide for its high surface sensitivity, adapted for measurements on non-ionic surfactants. It was specifically designed in an open-volume fluidic configuration for label-free investigations of artificial and biological membrane systems, in the gigahertz frequency regime. The experimental platform is flexible and can easily be integrated with other technologies, such as heating probes and fluidic arrangements. Moreover, the platform establishes a basis for advancing towards on-wafer measurements of the reflection and transmission parameters in the terahertz frequency regime.

In addition to the developments discussed in this thesis, there are numerous opportunities for other technological areas to contribute to investigations of biological entities. Examples include acoustophoresis, which has been integrated into fluidic devices, in order to concentrate cells and particles [196], as well as to remove proteins from blood plasma [197] and platelets from peripheral blood progenitor products [198]. Digital microfluidics is a surface-based technology, which performs discrete fluidic operations, such as transporting, splitting and mixing of droplets, on electrodes coated with a hydrophobic insulator. Recently, a proof-of-concept platform, for detection of rubella virus infection was demonstrated [199] in this area, and combination of digital microfluidics with impedance sensing for simultaneous cell culture and analysis has also been reported [200]. Moreover, nano-scale devices to address even smaller systems, DNA [201, 202] and proteins [203, 204], and micro-scale devices to study larger cellular organisms, nematodes [205] and fruit flies [206, 207], are also being successfully utilized.

Chapter 6. Summary of Results

6 Summary of Results

This chapter presents the summary of the papers included in this thesis. The experimental setups described within these papers find their primary use in the manipulation and patterning of single-cells in adherent cell cultures, with the exception of Paper IV, in which the potential of the platform was demonstrated on non-ionic surfactants.

6.1 Paper I

Cellular communication via directed protrusion growth: critical length-scales and membrane morphology

In order to study cellular communication, a previously reported method employed a micro-needle manipulation protocol for man-made network architectures involving biological cells. This work, however, presented a high risk of cell damage [1]. We were interested in controlling the formation of a natural network between adherent cells. For this purpose, we developed micropatterned substrates for directing cell growth, employing a photolithography-based surface fabrication strategy to produce Teflon AF structures on glass substrates. Teflon AF was selected for its cytophobic, but not cytotoxic, properties [87].

Paper I presents the investigation of the capability of cell protrusions from adherent Human Embryonic Kidney (HEK) 293 cells to bridge cytophobic Teflon AF microgaps. The frequency of cell protrusions crossing the cytophobic microgap was found to be strongly dependent on the gap size. Cell extensions crossing the gaps appeared either as nano-sized or micro-sized connections (see Figure 6.1). A free-standing microfluidic perfusion device, the multifunctional pipette (MFπ), was utilized for investigating molecular transport in the established cell-to-cell connections across the microgaps. One of the connected cells was selectively perfused with menthol to activate the TRPM8 ion channels overexpressed in the cells, followed by a supply of calcium ions. The diffusion of the calcium ions was visualized by means of a cell-permeant pre-fluorescent calcium-binding dye. Both open- and close-ended

intercellular connections in nano- and micro-sized protrusions were observed. At distances greater than 4 μm the occurrence of cell-to-cell connections was significantly reduced (see Figure 6.1E).

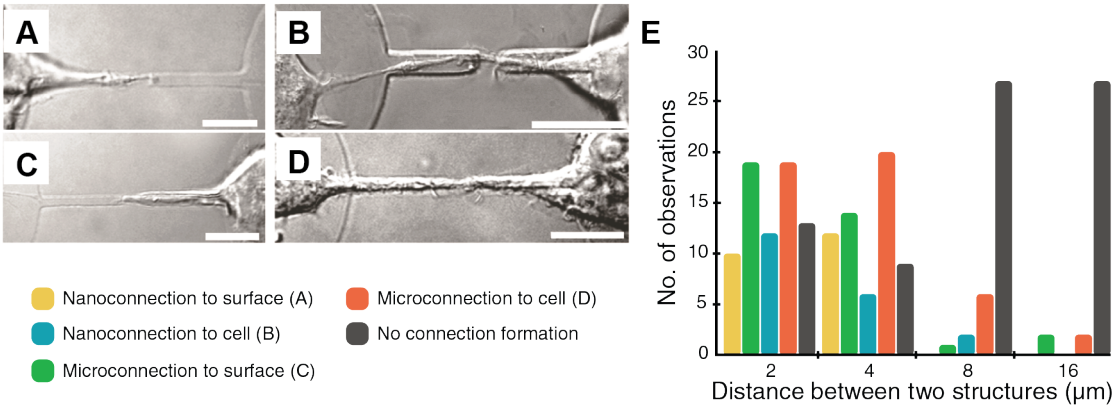

Figure 6.1: Cellular tubular growth of HEK 293 cells on Teflon AF patterned glass substrates. A-D) Bright-field images of the identified types of cellular connections. Scale bar 10 μm. E) A graph summarizing the total number of the different connections observed for microgaps of different lengths.

Keywords: adherent single cells, microfluidics, hydrodynamically confined flow, selective perfusion, cell-to-cell connections, Teflon AF, cell protrusions, molecular transport.

6.2 Paper II

A rapid microfluidic technique for integrated viability determination of adherent single cells

The recent increase in the interest of single-cell studies has led to the need for suitable techniques and instrumentation that can be used in conjunction with standard cell culture equipment and procedures. **Paper II** describes a novel protocol for rapid determination of viability of individual cells in an adherent cell culture, illustrated in Figure 6.2. We utilize a free-standing microfluidic perfusion device, the multifunctional pipette (MFπ), to create an isolated chemical environment around single cells.

The viability assay is combined with a cell poration experiment, in which cells are selectively exposed to the pore-forming agent digitonin, followed by fluorescein diphosphate (FDP, a pre-fluorescent substrate for alkaline phosphatase), in order to monitor intracellular enzyme

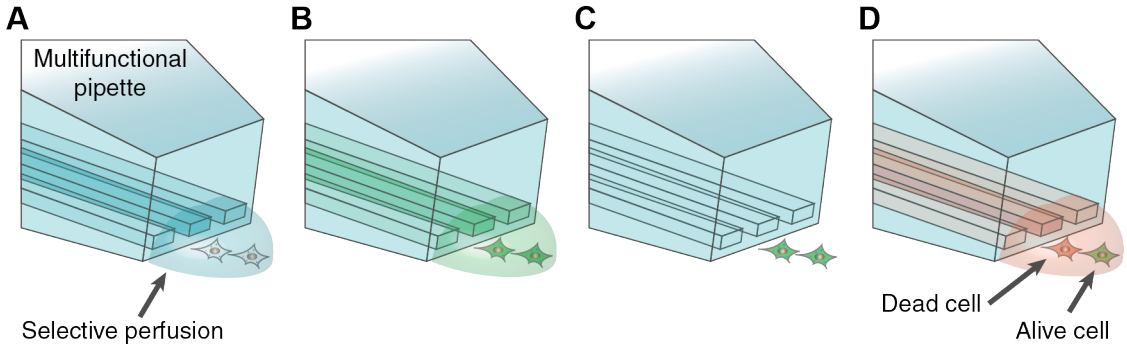

Figure 6.2: Schematic representation of the four sequential steps in the single-cell perfusion experiment. The target cells are selectively exposed to an isolated chemical environment created by the MFπ. A) The cells are exposed to the pore-forming agent, digitonin. B) The permeabilized cells are exposed to FDP to monitor enzyme activity. C) During a short resting period, the cell membrane is allowed to recover. D) The cell viability is assessed by simultaneous perfusion with FDA and PI. Fluorescence emission is recorded in the green (viable) and red (non-viable) channels, respectively.

activity by fluorescence microscopy. The viability was subsequently assessed through simultaneous perfusion with fluorescein diacetate (FDA) and propidium iodide (PI), in the same experiment. The microfluidic technology-assisted sequence of reagent delivery and viability test is a convenient and reliable single-cell approach, which avoids affecting the remaining cells in the culture. The test can be performed routinely alongside typical delivery protocols, and removes the need for global cell viability assays.

Keywords: adherent single cells, viability, microfluidics, hydrodynamically confined flow, selective perfusion, fluorescein diacetate (FDA), propidium iodide (PI).

6.3 Paper III

Free-standing SU-8 microfluidic probes

In order to enhance the performance and expand the application range of free-standing microfluidic probes, we developed a microfabrication process using a rigid photo-patternable material, SU-8. We utilize thermal release tape, a common cleanroom material, for a facile heat-release of the sacrificial layer from the support wafer. As a result, the fabricated microstructures can be released mechanically by gentle deformation of the thermal release tape.

Using the established procedure, illustrated in Figure 6.3, we demonstrated three practical implementations: i) a microfluidic probe, ii) a probe with integrated thin-film electrodes and

iii) a probe with perforated walls for microdialysis. The microfabrication process, described in **Paper III**, allows for high-yield batch production of versatile free-standing microfluidic devices in SU-8 with well-defined tip-geometry.

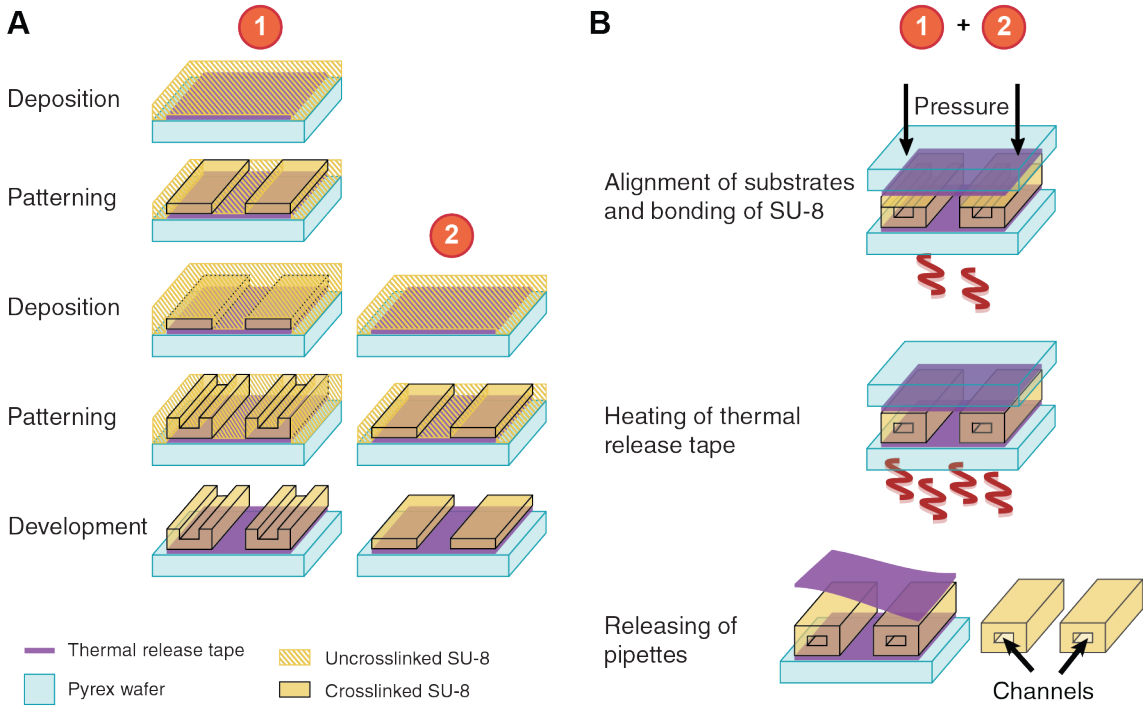

Figure 6.3: Schematic representation of the fabrication procedure of free-standing microfluidic devices with SU-8 epoxy, illustrating the use of the thermal release tape as the sacrificial layer. A) Simultaneous photolithographic processing of two wafers. B) Bonding and release procedure.

For characterization of the SU-8 microfluidic probes, two interfacing schemes were designed and tested: a disposable interface in PDMS with integrated wells, and an interface with external liquid reservoirs. The fabrication process was developed further to integrate electrodes on the surface of the SU-8 microfluidic probes, and an additional interface scheme, which incorporates electric components, was designed. We also investigated the possibilities of introducing perforations in the SU-8 device by photolithography. It was found that i) for micrometer-sized features an additional planarization step is crucial; ii) for probes with comparatively small dimensions (< 200 μm tip width), the mechanical release procedure is no longer feasible.

Keywords: microfluidics, hydrodynamically confined flow, selective perfusion, SU-8, thermal release tape, microfabrication, free-standing probes.

6.4 Paper IV

Millimeter-wave sensor based on a λ/2-line resonator for identification and dielectric characterization of non-ionic surfactants

We explored the possibility of using dielectric spectroscopy in the millimeter-wave region as an alternative label-free detection scheme for the study of biological and artificial membrane systems. Originally, the platform was developed for qualitative investigations of cholesterol content in model membranes [47]. In **Paper IV** the work was extended for characterization of two, structurally similar non-ionic surfactants (niosome constituents).

The novel open-volume millimeter-wave sensing platform is based on a coplanar waveguide (CPW). The experimental setup and the design of the sensor are illustrated in Figure 6.4.

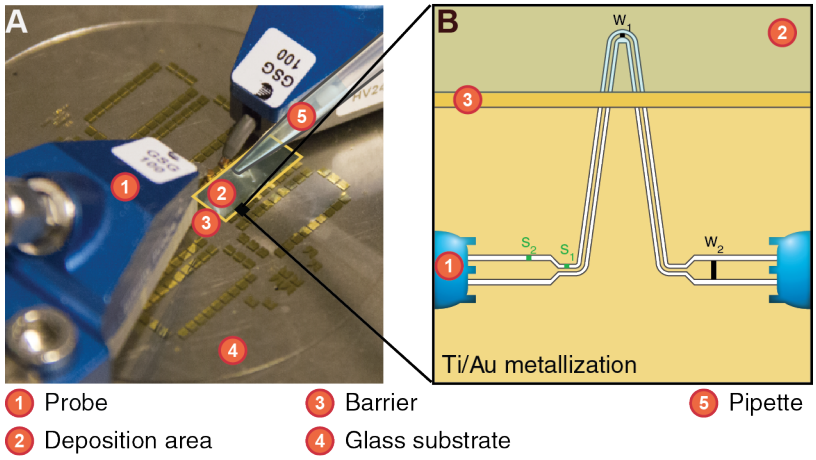

Figure 6.4: The sensor based on a coplanar waveguide. A) A photograph of the experimental setup. The deposition area is isolated by a barrier, and the black box represents one of the sensors. The pipette used to transfer the sample to the deposition area is also shown. B) A schematic representation of the sensor, illustrating the critical length scales w (signal width) and s (signal-to-ground) spacer: w_1, s_1, w_2 and s_2, are 10, 10, 50 and 14 μm, respectively.

The millimeter-wave sensor was implemented in an open-volume fluidic configuration to permit direct sample manipulation. Direct, on-wafer measurements of transmission and reflection parameters up to 110 GHz were performed. The sensor was capable of distinguishing

between the non-ionic surfactants Tween 20 and Span 80, due to a resonance shift of 3 GHz between the two compounds. Calibration structures for extraction of the complex permittivities were designed and fabricated.

Keywords: millimeter-waves, coplanar waveguide (CPW), open-volume fluidic configuration, niosomes, non-ionic surfactants, label-free.

Chapter 7. Concluding Remarks

7 Concluding Remarks

The work presented in this thesis focuses on the development of micro-scale platforms as a means to address some of the current challenges in the field of cell biology, related to the structure and function of single cells, and to provide bridging points between various novel technologies and the life sciences.

In **Paper I**, we have developed a platform for investigating intercellular communication through protrusions, achieved by directing the protrusion growth. The novel platform facilitates fundamental studies of cell-to-cell communication, cellular protrusions, and the dynamics of native cell environments. We chose to focus on the cells' capability to probe free-space in its immediate vicinity, and established a critical length-scale, beyond which this becomes increasingly difficult. A natural extension of the project would be to continuously monitor the formation of the micro- and nano-sized protrusions, and to characterize them in terms of protein content and actin organization. Moreover, in its current configuration, the platform investigates pairs of cells, however, establishing a larger network of interconnected cells in a controlled manner would enable exciting new possibilities of studying cell-to-cell communication.

Related to the studies in **Paper I** above, we have also developed a protocol for rapid assessment of cell viability, demonstrated in **Paper II**. The method enables selective viability testing of cells still under investigation, and the surrounding cells, prior to running a superfusion procedure. Both tests are not possible with conventional non-selective viability staining assays. This single-cell technique is thus complimentary to global cell screening. The established protocol is of particular interest in experimental setups which address cell heterogeneity, and is readily combined with other single-cell techniques, such as electrophysiology.

In **Paper III**, we presented a promising microfabrication process for SU-8 free-standing microfluidic probes, based on a sacrificial layer which enables an entirely mechanical release of the final structures. The use of SU-8 offers many benefits in terms of its chemical and

mechanical properties, scalability, and integration. It opens pathways to new microfluidic probes for life science applications useful for studying, among others, the pharmacological effects of drugs on cells and tissues. In addition, SU-8 permits easy integration with electric components, however, its autofluorescence limits its use in fluorescence microscopy environments. The material would find its ideal application in conventional optical microscopy and label-free experimental setups, where its autofluorescence would not be a relevant concern.

Current studies of biological and artificial membranes still rely heavily on the use of fluorescent tags, which often influence the system under investigation. For this reason, we explored the possibility of using dielectric spectroscopy, a non-invasive, label-free technique which can probe a sample in its native environment without the need for chemical modifications. This has led to the development of a mm-wave sensing platform, presented in **Paper IV**. This platform holds promise as a novel tool to improve the understanding of the properties of amphiphilic molecules, and the role of compositional variances. We consider it the first step towards real-time monitoring of biological structures. Moreover, such measurements have the potential to contribute to our understanding of the molecular interactions that occur in the GHz regime, and pave the way for investigations at even higher frequencies.

I am convinced that the work in this thesis has created new research opportunities, and will contribute to the deeper understanding of the fascinating nature of biological cells and their complex functions.

Acknowledgements

Acknowledgements

I would like to express my sincere gratitude to the following people:

My supervisors, thank you for giving me this opportunity! I have learned a lot in this process, and developed both academically and personally.
Aldo: for believing in me, for the fruitful discussions and for giving me the freedom to explore my own research ideas.
Kent: for all of your support and for the interesting discussions on neuropsychopharmacology. I hope we will have a chance to work together in the future.

My examiner, **Per**: for your meaningful input on my work.

Gavin: for your invaluable support and patience, and for the useful discussions and insight, during all of these years.

My co-authors: for great collaborations and your invaluable contributions to the projects. Thank you for the fascinating discussions on: **Alar** - microfluidics, **Helena** - millimeter- and sub-millimeter-waves, **Kiryl** - microfabrication and **Shijun** - biological cells.

Tanya: for your encouragement and assistance.

The MC2 lab crew, with special thanks to: **Johan**, **Henrik**, **Mats** and **Göran P.** for their extensive assistance.

The people in the division of chemistry and biochemistry, in particular, the past and the present members of the research group. Thank you for the interesting discussions and the amazing work environment!

My wonderful friends: **Celine**, **Emelie**, **Kiryl**, **Natasha**, **Laura**, **Satomi**, **Mai**, **Nicki**, **Jocce** and **Maria**. Thank you for all the good memories!

Luca: per tutto il tuo sostegno e incoraggiamento, per il tuo brio e magnifico senso dell'umorismo. Sopratutto per aver cucinato deliziosi piatti, durante le lunghe sere di scrittura di questa tesi, e non.

И, конечно же, мою семью. В частности, моих родителей, за их невероятную поддержку, понимание и любовь. Я знаю, что я не сделала бы это без вас!

Bibliography

Bibliography

[1] H. Zhang, S. Xu, G. D. Jeffries, O. Orwar, and A. Jesorka, "Artificial nanotube connections and transport of molecular cargo between mammalian cells," *Nano Communication Networks*, vol. 4, no. 4, pp. 197–204, 2013.

[2] B. Alberts, A. Johnson, J. Lewis, M. Raff, K. Roberts, and P. Walter, *Molecular Biology of the Cell*. Garland Publishing Inc, 5th ed., 2008.

[3] G. Bao and S. Suresh, "Cell and molecular mechanics of biological materials," *Nature Materials*, vol. 2, pp. 715–725, nov 2003.

[4] N. Ramkumar and B. Baum, "Coupling changes in cell shape to chromosome segregation," *Nature Reviews Molecular Cell Biology*, jun 2016.

[5] C. F. Ehret, "Organelle systems and biological organization. Structural and developmental evidence leads to a new look at our concepts of biological organization.," *Science (New York, N.Y.)*, vol. 132, pp. 115–23, jul 1960.

[6] N. W. Goehring and A. A. Hyman, "Organelle Growth Control through Limiting Pools of Cytoplasmic Components," *Current Biology*, vol. 22, no. 9, pp. R330–R339, 2012.

[7] Y.-H. M. Chan and W. F. Marshall, "How cells know the size of their organelles.," *Science (New York, N.Y.)*, vol. 337, pp. 1186–9, sep 2012.

[8] V. Rottiers and A. M. Näär, "MicroRNAs in metabolism and metabolic disorders," *Nature Reviews Molecular Cell Biology*, vol. 13, pp. 239–250, mar 2012.

[9] R. A. Cairns, I. S. Harris, and T. W. Mak, "Regulation of cancer cell metabolism," *Nature Reviews Cancer*, vol. 11, pp. 85–95, feb 2011.

[10] D. R. Green, L. Galluzzi, and G. Kroemer, "Cell biology. Metabolic control of cell death.," *Science (New York, N.Y.)*, vol. 345, p. 1250256, sep 2014.

[11] A. Rustom, R. Saffrich, I. Markovic, P. Walther, and H.-H. Gerdes, "Nanotubular highways for intercellular organelle transport.," *Science (New York, N.Y.)*, vol. 303, pp. 1007–10, feb 2004.

[12] M. M. Matzuk, K. H. Burns, M. M. Viveiros, and J. J. Eppig, "Intercellular communication in the mammalian ovary: oocytes carry the conversation.," *Science (New York, N.Y.)*, vol. 296, pp. 2178–80, jun 2002.

[13] L. N. Handly, A. Pilko, and R. Wollman, "Paracrine communication maximizes cellular response fidelity in wound signaling.," *eLife*, vol. 4, p. e09652, 2015.

[14] C. C. Yap and B. Winckler, "Harnessing the Power of the Endosome to Regulate Neural Development," *Neuron*, vol. 74, no. 3, pp. 440–451, 2012.

[15] B.-Z. Shilo and E. D. Schejter, "Regulation of developmental intercellular signalling by intracellular trafficking.," *The EMBO journal*, vol. 30, pp. 3516–26, aug 2011.

[16] Y. Fuchs and H. Steller, "Live to die another way: modes of programmed cell death and the signals emanating from dying cells," *Nature Reviews Molecular Cell Biology*, vol. 16, pp. 329–344, may 2015.

[17] C. Aguirre-Chen and C. M. Hammell, "Cell death machinery makes life more robust.," *eLife*, vol. 3, p. e05816, 2014.

[18] S. V. Avery, "Microbial cell individuality and the underlying sources of heterogeneity," *Nature Reviews Microbiology*, vol. 4, pp. 577–587, aug 2006.

[19] M. Wu and A. K. Singh, "Single-cell protein analysis," *Current Opinion in Biotechnology*, vol. 23, no. 1, pp. 83–88, 2012.

[20] S. Gavasso, S.-E. Gullaksen, J. Skavland, and B. T. Gjertsen, "Single-cell proteomics: potential implications for cancer diagnostics," *Expert Review of Molecular Diagnostics*, vol. 16, pp. 579–589, may 2016.

[21] C. Denef, "Paracrinicity: the story of 30 years of cellular pituitary crosstalk.," *Journal of neuroendocrinology*, vol. 20, pp. 1–70, jan 2008.

[22] S. J. Singer, "Intercellular communication and cell-cell adhesion.," *Science (New York, N.Y.)*, vol. 255, pp. 1671–7, mar 1992.

[23] J. E. Trosko and R. J. Ruch, "Cell-cell communication in carcinogenesis.," *Frontiers in bioscience : a journal and virtual library*, vol. 3, pp. d208–36, feb 1998.

[24] P. K. Mattila and P. Lappalainen, "Filopodia: molecular architecture and cellular functions.," *Nature reviews. Molecular cell biology*, vol. 9, no. 6, pp. 446–454, 2008.

[25] M. J. Lehmann, N. M. Sherer, C. B. Marks, M. Pypaert, and W. Mothes, "Actin- and myosin-driven movement of viruses along filopodia precedes their entry into cells," *The Journal of Cell Biology*, vol. 170, no. 2, 2005.

[26] Z. U. Rehman, K. A. Sjollema, J. Kuipers, D. Hoekstra, and I. S. Zuhorn, "Nonviral gene delivery vectors use syndecan-dependent transport mechanisms in filopodia to reach the cell surface," *ACS Nano*, vol. 6, pp. 7521–7532, aug 2012.

[27] A. Arjonen, R. Kaukonen, and J. Ivaska, "Filopodia and adhesion in cancer cell motility," *Cell Adhesion and Migration*, vol. 5, no. 5, 2011.

[28] T. Bornschlögl, "How filopodia pull: What we know about the mechanics and dynamics of filopodia," *Cytoskeleton*, vol. 70, no. 10, pp. 590–603, 2013.

[29] M. J. Stoddart, ed., *Mammalian Cell Viability*, vol. 740 of *Methods in Molecular Biology*. Totowa, NJ: Humana Press, 2011.

[30] R. S. Franco, "Measurement of red cell lifespan and aging.," *Transfusion medicine and hemotherapy*, vol. 39, pp. 302–7, oct 2012.

[31] M.-H. Cho, A. Niles, R. Huang, J. Inglese, C. P. Austin, T. Riss, and M. Xia, "A bioluminescent cytotoxicity assay for assessment of membrane integrity using a proteolytic biomarker.," *Toxicology in vitro*, vol. 22, pp. 1099–106, jun 2008.

[32] L. Kupcsik, "Estimation of cell number based on metabolic activity: the MTT reduction assay.," *Methods in Molecular Biology*, vol. 740, pp. 13–9, 2011.

[33] W. Strober, "Trypan blue exclusion test of cell viability.," *Current protocols in immunology*, p. Appendix 3B, may 2001.

[34] L. Braydich-Stolle, S. Hussain, J. J. Schlager, and M.-C. Hofmann, "In vitro cytotoxicity of nanoparticles in mammalian germline stem cells.," *Toxicological sciences*, vol. 88, pp. 412–9, dec 2005.

[35] L. A. Castro-Concha, R. M. Escobedo, and M. de Lourdes Miranda-Ham, "Measurement of Cell Viability in In Vitro Cultures," in *Plant Cell Culture Protocols*, pp. 071–076, New Jersey: Humana Press, 2006.

[36] A. Krishan, "Rapid flow cytofluorometric analysis of mammalian cell cycle by propidium iodide staining," *The Journal of Cell Biology*, vol. 66, pp. 188–193, jul 1975.

[37] K. H. Jones and J. A. Senft, "An improved method to determine cell viability by simultaneous staining with fluorescein diacetate-propidium iodide.," *Journal of Histochemistry & Cytochemistry*, vol. 33, pp. 77–79, jan 1985.

[38] M. Ramanathan, L. K. Shrestha, T. Mori, Q. Ji, J. P. Hill, and K. Ariga, "Amphiphile nanoarchitectonics: from basic physical chemistry to advanced applications," *Physical Chemistry Chemical Physics*, vol. 15, no. 26, p. 10580, 2013.

[39] D. D. Lasic, "Novel applications of liposomes," *Trends in Biotechnology*, vol. 16, no. 7, pp. 307–321, 1998.

[40] K. Egbaria and N. Weiner, "Liposomes as a topical drug delivery system," *Advanced Drug Delivery Reviews*, vol. 5, no. 3, pp. 287–300, 1990.

[41] K. Holmberg, B. Jönsson, B. Kronberg, and B. Lindman, *Surfactants and polymers in aqueous solution.* John Wiley & Sons, 2003.

[42] G. P. Kumar and P. Rajeshwarrao, "Nonionic surfactant vesicular systems for effective drug delivery—an overview," *Acta Pharmaceutica Sinica B*, vol. 1, no. 4, pp. 208–219, 2011.

[43] J. Jiao, "Polyoxyethylated nonionic surfactants and their applications in topical ocular drug delivery," *Advanced Drug Delivery Reviews*, vol. 60, no. 15, pp. 1663–1673, 2008.

[44] C. Dufes, F. Gaillard, I. F. Uchegbu, A. G. Schätzlein, J.-C. Olivier, and J.-M. Muller, "Glucose-targeted niosomes deliver vasoactive intestinal peptide (VIP) to the brain," *International Journal of Pharmaceutics*, vol. 285, no. 1, pp. 77–85, 2004.

[45] N. B. Mahale, P. D. Thakkar, R. G. Mali, D. R. Walunj, and S. R. Chaudhari, "Niosomes: Novel sustained release nonionic stable vesicular systems - An overview," *Advances in Colloid and Interface Science*, vol. 183-184, pp. 46–54, 2012.

[46] S. Moghassemi and A. Hadjizadeh, "Nano-niosomes as nanoscale drug delivery systems: An illustrated review," *Journal of Controlled Release*, vol. 185, pp. 22–36, 2014.

[47] A. Kim, H. Rodilla, G. Jeffries, J. Vukusic, J. Stake, and A. Jesorka, "Label-free millimeter-wave sensor for investigations of biological model membrane systems," in *MicroTAS 2015 - 19th International Conference on Miniaturized Systems for Chemistry and Life Sciences*, 2015.

[48] M. J. Madou, *Fundamentals of microfabrication and nanotechnology*. CRC Press, 3rd ed., 2012.

[49] M. J. Madou, *Fundamentals of microfabrication : the science of miniaturization*. CRC Press, 2nd ed., 2002.

[50] A. Kumar and G. M. Whitesides, "Features of gold having micrometer to centimeter dimensions can be formed through a combination of stamping with an elastomeric stamp and an alkanethiol "ink" followed by chemical etching," *Applied Physics Letters*, vol. 63, no. 14, p. 2002, 1993.

[51] Y. Xia, J. J. McClelland, R. Gupta, D. Qin, X.-M. Zhao, L. L. Sohn, R. J. Celotta, and G. M. Whitesides, "Replica molding using polymeric materials: A practical step toward nanomanufacturing," *Advanced Materials*, vol. 9, pp. 147–149, feb 1997.

[52] X.-M. Zhao, Y. Xia, and G. M. Whitesides, "Fabrication of three-dimensional microstructures: Microtransfer molding," *Advanced Materials*, vol. 8, pp. 837–840, oct 1996.

[53] E. Kim, Y. Xia, and G. M. Whitesides, "Polymer microstructures formed by moulding in capillaries," *Nature*, vol. 376, pp. 581–584, aug 1995.

[54] Z. Li, Y. Gu, L. Wang, H. Ge, W. Wu, Q. Xia, C. Yuan, Y. Chen, B. Cui, and R. S. Williams, "Hybrid Nanoimprint-Soft Lithography with Sub-15 nm Resolution," 2009.

[55] A. Chand, M. Viani, T. Schaffer, and P. Hansma, "Microfabricated small metal cantilevers with silicon tip for atomic force microscopy," *Journal of Microelectromechanical Systems*, vol. 9, pp. 112–116, mar 2000.

[56] C. Duan, W. Wang, and Q. Xie, "Review article: Fabrication of nanofluidic devices.," *Biomicrofluidics*, vol. 7, p. 26501, mar 2013.

[57] S. K. Sia and G. M. Whitesides, "Microfluidic devices fabricated in Poly(dimethylsiloxane) for biological studies," *Electrophoresis*, vol. 24, pp. 3563–3576, nov 2003.

[58] John L. Tan, , Joe Tien, and C. S. Chen*, "Microcontact Printing of Proteins on Mixed Self-Assembled Monolayers," 2001.

[59] H.-Y. Lin, C.-Y. Hsu, J. L. Thomas, S.-E. Wang, and H.-C. Chen, "The microcontact imprinting of proteins: The effect of cross-linking monomers for lysozyme, ribonuclease A and myoglobin," *Biosensors and Bioelectronics*, vol. 22, no. 4, pp. 534–543, 2006.

[60] R. S. Kane, S. Takayama, E. Ostuni, D. E. Ingber, and G. M. Whitesides, "Patterning proteins and cells using soft lithography," *Biomaterials*, vol. 20, no. 23, pp. 2363–2376, 1999.

[61] J. A. Rogers, Z. Bao, and V. R. Raju, "Nonphotolithographic fabrication of organic transistors with micron feature sizes," *Applied Physics Letters*, vol. 72, no. 21, p. 2716, 1998.

[62] P. Cosseddu and A. Bonfiglio, "Soft lithography fabrication of all-organic bottom-contact and top-contact field effect transistors," *Applied Physics Letters*, vol. 88, no. 2, p. 023506, 2006.

[63] M. Jenik, A. Seifner, P. Lieberzeit, and F. L. Dickert, "Pollen-imprinted polyurethanes for QCM allergen sensors.," *Analytical and bioanalytical chemistry*, vol. 394, pp. 523–8, may 2009.

[64] J. Dong, N. Gao, Y. Peng, C. Guo, Z. Lv, Y. Wang, C. Zhou, B. Ning, M. Liu, and Z. Gao, "Surface plasmon resonance sensor for profenofos detection using molecularly imprinted thin film as recognition element," *Food Control*, vol. 25, no. 2, pp. 543–549, 2012.

[65] S. Franssila, *Introduction to microfabrication*. John Wiley & Sons, 2010.

[66] M. Agirregabiria, F. J. Blanco, J. Berganzo, M. T. Arroyo, a. Fullaondo, K. Mayora, and J. M. Ruano-López, "Fabrication of SU-8 multilayer microstructures based on successive CMOS compatible adhesive bonding and releasing steps.," *Lab on a chip*, vol. 5, no. 5, pp. 545–552, 2005.

[67] E. Mitri, G. Birarda, L. Vaccari, S. Kenig, M. Tormen, and G. Grenci, "SU-8 bonding protocol for the fabrication of microfluidic devices dedicated to FTIR microspectroscopy of live cells.," *Lab on a chip*, vol. 14, no. 1, pp. 210–8, 2014.

[68] K. Malachowski, M. Jamal, Q. Jin, B. Polat, C. J. Morris, and D. H. Gracias, "Self-folding single cell grippers," *Nano Letters*, vol. 14, no. 7, pp. 4164–4170, 2014.

[69] S.-W. Lee, M. Muoth, T. Helbling, M. Mattmann, and C. Hierold, "Suppression of resist contamination during photolithography on carbon nanomaterials by a sacrificial layer," *Carbon*, vol. 66, pp. 295–301, 2014.

[70] J. M. Weisse, C. H. Lee, D. R. Kim, L. Cai, P. M. Rao, and X. Zheng, "Electroassisted Transfer of Vertical Silicon Wire Arrays Using a Sacrificial Porous Silicon Layer," 2013.

[71] S.-H. Chuang, C.-T. Pan, K.-C. Shen, S.-L. Ou, D.-S. Wuu, and R.-H. Horng, "Thin Film GaN LEDs Using a Patterned Oxide Sacrificial Layer by Chemical Lift-Off Process," *IEEE Photonics Technology Letters*, vol. 25, pp. 2435–2438, dec 2013.

[72] C. David, J. Bruder, T. Rohbeck, C. Grünzweig, C. Kottler, A. Diaz, O. Bunk, and F. Pfeiffer, "Fabrication of diffraction gratings for hard X-ray phase contrast imaging," *Microelectronic Engineering*, vol. 84, no. 5, pp. 1172–1177, 2007.

[73] Y. Sun and Y. Xia, "Triangular Nanoplates of Silver: Synthesis, Characterization, and Use as Sacrificial Templates For Generating Triangular Nanorings of Gold," *Advanced Materials*, vol. 15, pp. 695–699, may 2003.

[74] Z. Cui and R. A. Lawes, "A new sacrificial layer process for the fabrication of micromechanical systems," *Journal of Micromechanics and Microengineering*, vol. 7, pp. 128–130, sep 1997.

[75] C. Chung and M. Allen, "Uncrosslinked SU-8 as a sacrificial material," *Journal of Micromechanics and Microengineering*, vol. 15, no. 1, pp. N1–N5, 2004.

[76] I. Pinnau and L. G. Toy, "Gas and vapor transport properties of amorphous perfluorinated copolymer membranes based on 2,2-bistrifluoromethyl-4,5-difluoro-1,3-dioxole/tetrafluoroethylene," *Journal of Membrane Science*, vol. 109, no. 1, pp. 125–133, 1996.

[77] L. D. Hughes and T. A. DeVol, "Characterization of a Teflon coated semiconductor detector flow cell for monitoring of pertechnetate in groundwater," *Journal of Radioanalytical and Nuclear Chemistry*, vol. 267, pp. 287–295, jan 2006.

[78] M. Osterfeld, H. Franke, and C. Feger, "Optical gas detection using metal film enhanced leaky mode spectroscopy," *Applied Physics Letters*, vol. 62, no. 19, p. 2310, 1993.

[79] J. Harwood, "TEFLON AF-A new polymer for electronics," in *8th IEEE/CHMT International Conference on Electronic Manufacturing Technology Symposium*, pp. 503–507, IEEE, 1990.

[80] N. Fukutake, N. Miyoshi, Y. Takasawa, T. Urakawa, T. Gowa, K. Okamoto, A. Oshima, S. Tagawa, and M. Washio, "Micro- and Nano-Scale Fabrication of Fluorinated Polymers by Direct Etching Using Focused Ion Beam," *Japanese Journal of Applied Physics*, vol. 49, p. 065201, jun 2010.

[81] Y. Zhang, T. Katoh, M. Washio, H. Yamada, and S. Hamada, "High aspect ratio micromachining Teflon by direct exposure to synchrotron radiation," *Applied Physics Letters*, vol. 67, no. 6, p. 872, 1995.

[82] T. Katoh, N. Nishi, M. Fukagawa, H. Ueno, and S. Sugiyama, "Direct writing for three-dimensional microfabrication using synchrotron radiation etching," *Sensors and Actuators A: Physical*, vol. 89, no. 1, pp. 10–15, 2001.

[83] K. Ren, W. Dai, J. Zhou, J. Su, and H. Wu, "Whole-Teflon microfluidic chips," *Proceedings of the National Academy of Sciences*, vol. 108, no. 20, pp. 8162–8166, 2011.

[84] V. Karre, P. D. Keathley, J. Guo, and J. T. Hastings, "Direct Electron-Beam Patterning of Teflon AF," *IEEE transactions on nanotechnology*, vol. 8, no. 2, pp. 139–141, 2009.

[85] M. Shaali, S. Lara-Avila, P. Dommersnes, A. Ainla, S. Kubatkin, and A. Jesorka, "Nanopatterning of Mobile Lipid Monolayers on Electron-Beam-Sculpted Teflon AF Surfaces," *ACS Nano*, vol. 9, pp. 1271–1279, feb 2015.

[86] I. Czolkos, B. Hakonen, O. Orwar, and A. Jesorka, "High-resolution micropatterned Teflon AF substrates for biocompatible nanofluidic devices," *Langmuir*, vol. 28, no. 6, pp. 3200–3205, 2012.

[87] S. Makohliso, L. Giovangrandi, D. Léonard, H. Mathieu, M. Ilegems, and P. Aebischer, "Application of Teflon-AF® thin films for bio-patterning of neural cell adhesion," *Biosensors and Bioelectronics*, vol. 13, no. 11, pp. 1227–1235, 1998.

[88] C. C. Anamelechi, G. A. Truskey, and W. M. Reichert, "Mylar™ and Teflon-AF™ as cell culture substrates for studying endothelial cell adhesion," *Biomaterials*, vol. 26, no. 34, pp. 6887–6896, 2005.

[89] F. Valle, B. Chelli, M. Bianchi, P. Greco, E. Bystrenova, I. Tonazzini, and F. Biscarini, "Stable Non-Covalent Large Area Patterning of Inert Teflon-AF Surface: A New Approach to Multiscale Cell Guidance," *Advanced Engineering Materials*, vol. 12, pp. B185–B191, jun 2010.

[90] B. Shen, B. Xiong, and H. Wu, "Convenient surface functionalization of whole-Teflon chips with polydopamine coating," *Biomicrofluidics*, vol. 9, no. 4, p. 044111, 2015.

[91] X. Shi, S. Chen, J. Zhou, H. Yu, L. Li, and H. Wu, "Directing Osteogenesis of Stem Cells with Drug-Laden, Polymer-Microsphere-Based Micropatterns Generated by Teflon Microfluidic Chips," *Advanced Functional Materials*, vol. 22, pp. 3799–3807, sep 2012.

[92] T. W. de Haas, H. Fadaei, and D. Sinton, "Laminated thin-film Teflon chips for petrochemical applications," *Lab on a Chip*, vol. 12, no. 21, p. 4236, 2012.

[93] MicroChem Corp, "MicroChem Negative Epoxy Resists."

[94] C.-J. Chang, C.-S. Yang, Y.-J. Chuang, H.-S. Khoo, and F.-G. Tseng, "Micropatternable nanoporous polymer integrated with microstructures for molecular filtration.," *Nanotechnology*, vol. 19, no. 36, p. 365301, 2008.

[95] S. Keller, G. Blagoi, M. Lillemose, D. Haefliger, and A. Boisen, "Processing of thin SU-8 films," *Journal of Micromechanics and Microengineering*, vol. 18, no. 12, p. 125020, 2008.

[96] M. A. Uddin, H. P. Chan, C. K. Chow, and Y. C. Chan, "Effect of spin coating on the curing rate of epoxy adhesive for the fabrication of a polymer optical waveguide," *Journal of Electronic Materials*, vol. 33, pp. 224–228, mar 2004.

[97] A. del Campo and C. Greiner, "SU-8: a photoresist for high-aspect-ratio and 3D submicron lithography," *Journal of Micromechanics and Microengineering*, vol. 17, no. 6, pp. R81–R95, 2007.

[98] R. Martinez-Duarte and M. J. Madou, "SU-8 photolithography and its impact on microfluidics," 2011.

[99] H. Lorenz, M. Despont, N. Fahrni, J. Brugger, P. Vettiger, and P. Renaud, "High-aspect-ratio, ultrathick, negative-tone near-UV photoresist and its applications for MEMS," *Sensors and Actuators A: Physical*, vol. 64, pp. 33–39, jan 1998.

[100] R. Yang and W. Wang, "A numerical and experimental study on gap compensation and wavelength selection in UV-lithography of ultra-high aspect ratio SU-8 microstructures," *Sensors and Actuators B: Chemical*, vol. 110, no. 2, pp. 279–288, 2005.

[101] A. Mata, A. J. Fleischman, and S. Roy, "Fabrication of multi-layer SU-8 microstructures," *Journal of Micromechanics and Microengineering*, vol. 16, pp. 276–284, feb 2006.

[102] A. Altuna, E. Bellistri, E. Cid, P. Aivar, B. Gal, J. Berganzo, G. Gabriel, A. Guimerà, R. Villa, L. J. Fernández, and L. Menendez de la Prida, "SU-8 based microprobes for simultaneous neural depth recording and drug delivery in the brain.," *Lab on a chip*, vol. 13, no. 7, pp. 1422–30, 2013.

[103] T. C. Leïchlé, M. V. Arx, S. Reiman, I. Zana, W. Ye, and M. G. Allen, "A low-power resonant micromachined compass," *Journal of Micromechanics and Microengineering*, vol. 14, pp. 462–470, apr 2004.

[104] S. Tuomikoski and S. Franssila, "Free-standing SU-8 microfluidic chips by adhesive bonding and release etching," *Sensors and Actuators A: Physical*, vol. 120, no. 2, pp. 408–415, 2005.

[105] W. W. Chi, W. W. Seng, L. K. Siong, I. A. Azid, K. Ibrahim, and D. Mutharasu, "Dry release of SU-8 structures using OHP transparency as the substrate material," *Sensors and Actuators, A: Physical*, vol. 167, no. 1, pp. 97–101, 2011.

[106] R. Vilares, C. Hunter, I. Ugarte, I. Aranburu, J. Berganzo, J. Elizalde, and L. J. Fernandez, "Fabrication and testing of a SU-8 thermal flow sensor," *Sensors and Actuators, B: Chemical*, vol. 147, no. 2, pp. 411–417, 2010.

[107] P. Abgrall, C. Lattes, V. Conédéra, X. Dollat, S. Colin, and A. M. Gué, "A novel fabrication method of flexible and monolithic 3D microfluidic structures using lamination of SU-8 films," *Journal of Micromechanics and Microengineering*, vol. 16, no. 1, pp. 113–121, 2005.

[108] G. Petit-Pierre, A. Bertsch, and P. Renaud, "Neural probe combining microelectrodes and a droplet-based microdialysis collection system for high temporal resolution sampling," *Lab Chip*, vol. 16, pp. 917–924, feb 2016.

[109] C. Luo, A. Govindaraju, J. Garra, T. Schneider, R. White, J. Currie, and M. Paranjape, "Releasing SU-8 structures using polystyrene as a sacrificial material," *Sensors and Actuators, A: Physical*, vol. 114, no. 1, pp. 123–128, 2004.

[110] J. N. Patel, B. Kaminska, B. L. Gray, and B. D. Gates, "PDMS as a sacrificial substrate for SU-8-based biomedical and microfluidic applications," *Journal of Micromechanics and Microengineering*, vol. 18, no. 9, p. 095028, 2008.

[111] B. Bohl, R. Steger, R. Zengerle, and P. Koltay, "Multi-layer SU-8 lift-off technology for microfluidic devices," *Journal of Micromechanics and Microengineering*, vol. 15, no. 6, pp. 1125–1130, 2005.

[112] D. Pesántez, E. Amponsah, and A. Gadre, "Wet release of multipolymeric structures with a nanoscale release layer," *Sensors and Actuators B: Chemical*, vol. 132, no. 2, pp. 426–430, 2008.

[113] Z. Gao, D. B. Henthorn, and C.-S. Kim, "Enhanced wettability of SU-8 photoresist through a photografting procedure for bioanalytical device applications.," *Journal of micromechanics and microengineering : structures, devices, and systems*, vol. 18, pp. 450131–450137, jan 2008.

[114] F. Walther, P. Davydovskaya, S. Zürcher, M. Kaiser, H. Herberg, A. M. Gigler, and R. W. Stark, "Stability of the hydrophilic behavior of oxygen plasma activated SU-8," *Journal of Micromechanics and Microengineering*, vol. 17, pp. 524–531, mar 2007.

[115] M. Nordström, R. Marie, M. Calleja, and A. Boisen, "Rendering SU-8 hydrophilic to facilitate use in micro channel fabrication," *Journal of Micromechanics and Microengineering*, vol. 14, pp. 1614–1617, dec 2004.

[116] C. Wu, M. Chen, and F. Tseng, "SU-8 hydrophilic modification by forming copolymer with hydrophilic epoxy molecule," in *7th International Conference on Miniaturized Chemical and Biochemical Analysis Systems*, (Squaw Valley, CA, USA), pp. 1117–1120, 2003.

[117] K. V. Nemani, K. L. Moodie, J. B. Brennick, A. Su, and B. Gimi, "In vitro and in vivo evaluation of SU-8 biocompatibility," *Materials Science and Engineering: C*, vol. 33, no. 7, pp. 4453–4459, 2013.

[118] B. S. Rubin, "Bisphenol A: An endocrine disruptor with widespread exposure and multiple effects," *The Journal of Steroid Biochemistry and Molecular Biology*, vol. 127, no. 1, pp. 27–34, 2011.

[119] N. Chronis and L. Lee, "Electrothermally activated SU-8 microgripper for single cell manipulation in solution," *Journal of Microelectromechanical Systems*, vol. 14, pp. 857–863, aug 2005.

[120] J. C. Doll, N. Harjee, N. Klejwa, R. Kwon, S. M. Coulthard, B. Petzold, M. B. Goodman, and B. L. Pruitt, "SU-8 force sensing pillar arrays for biological measurements," *Lab on a Chip*, vol. 9, no. 10, p. 1449, 2009.

[121] J. H. Koschwanez, R. H. Carlson, and D. R. Meldrum, "Thin PDMS Films Using Long Spin Times or Tert-Butyl Alcohol as a Solvent," *PLoS ONE*, vol. 4, p. e4572, feb 2009.

[122] S. Wang, A. Kallur, and A. Goshu, "Fabrication and characterization of PDMS thin film," p. 79350M, International Society for Optics and Photonics, feb 2011.

[123] A. Thangawng, M. Swartz, M. Glucksberg, and R. S. Ruoff, "Bond–Detach Lithography: A Method for Micro/Nanolithography by Precision PDMS Patterning," *Small*, vol. 3, pp. 132–138, jan 2007.

[124] D. T. Eddington, J. P. Puccinelli, and D. J. Beebe, "Thermal aging and reduced hydrophobic recovery of polydimethylsiloxane," *Sensors and Actuators B: Chemical*, vol. 114, no. 1, pp. 170–172, 2006.

[125] D. C. Duffy, J. C. McDonald, O. J. A. Schueller, and G. M. Whitesides, "Rapid Prototyping of Microfluidic Systems in Poly(dimethylsiloxane)," *Analytical Chemistry*, vol. 70, pp. 4974–4984, dec 1998.

[126] S. Rosset, M. Niklaus, P. Dubois, and H. R. Shea, "Metal Ion Implantation for the Fabrication of Stretchable Electrodes on Elastomers," *Advanced Functional Materials*, vol. 19, pp. 470–478, feb 2009.

[127] J. N. Lee, C. Park, and G. M. Whitesides, "Solvent Compatibility of Poly(dimethylsiloxane)-Based Microfluidic Devices," *Analytical Chemistry*, vol. 75, pp. 6544–6554, dec 2003.

[128] M. A. Unger, H.-P. Chou, T. Thorsen, A. Scherer, and S. R. Quake, "Monolithic Microfabricated Valves and Pumps by Multilayer Soft Lithography," *Science*, vol. 288, no. 5463, 2000.

[129] M. He, J. S. Edgar, G. D. M. Jeffries, R. M. Lorenz, J. P. Shelby, and D. T. Chiu, "Selective Encapsulation of Single Cells and Subcellular Organelles into Picoliter- and Femtoliter-Volume Droplets," *Analytical Chemistry*, vol. 77, pp. 1539–1544, mar 2005.

[130] D. A. Czaplewski, J. Kameoka, R. Mathers, G. W. Coates, and H. G. Craighead, "Nanofluidic channels with elliptical cross sections formed using a nonlithographic process," *Applied Physics Letters*, vol. 83, no. 23, p. 4836, 2003.

[131] J. W. Hong and S. R. Quake, "Integrated nanoliter systems," *Nature Biotechnology*, vol. 21, pp. 1179–1183, oct 2003.

[132] J. K. W. Yang, Y. S. Jung, J.-B. Chang, R. A. Mickiewicz, A. Alexander-Katz, C. A. Ross, and K. K. Berggren, "Complex self-assembled patterns using sparse commensurate templates with locally varying motifs," *Nature Nanotechnology*, vol. 5, pp. 256–260, apr 2010.

[133] M. Théry, V. Racine, A. Pépin, M. Piel, Y. Chen, J.-B. Sibarita, and M. Bornens, "The extracellular matrix guides the orientation of the cell division axis," *Nature Cell Biology*, vol. 7, pp. 947–953, oct 2005.

[134] N. Wang, E. Ostuni, G. M. Whitesides, and D. E. Ingber, "Micropatterning tractional forces in living cells," *Cell Motility and the Cytoskeleton*, vol. 52, pp. 97–106, jun 2002.

[135] R. F. Shepherd, F. Ilievski, W. Choi, S. A. Morin, A. A. Stokes, A. D. Mazzeo, X. Chen, M. Wang, and G. M. Whitesides, "Multigait soft robot," *Proceedings of the National Academy of Sciences*, vol. 108, pp. 20400–20403, dec 2011.

[136] J. C. Nawroth, H. Lee, A. W. Feinberg, C. M. Ripplinger, M. L. McCain, A. Grosberg, J. O. Dabiri, and K. K. Parker, "A tissue-engineered jellyfish with biomimetic propulsion," *Nature Biotechnology*, vol. 30, pp. 792–797, jul 2012.

[137] S.-J. Park, M. Gazzola, K. S. Park, S. Park, V. Di Santo, E. L. Blevins, J. U. Lind, P. H. Campbell, S. Dauth, A. K. Capulli, F. S. Pasqualini, S. Ahn, A. Cho, H. Yuan, B. M.

Maoz, R. Vijaykumar, J.-W. Choi, K. Deisseroth, G. V. Lauder, L. Mahadevan, and K. K. Parker, "Phototactic guidance of a tissue-engineered soft-robotic ray.," *Science (New York, N.Y.)*, vol. 353, pp. 158–62, jul 2016.

[138] C. D. Chin, T. Laksanasopin, Y. K. Cheung, D. Steinmiller, V. Linder, H. Parsa, J. Wang, H. Moore, R. Rouse, G. Umviligihozo, E. Karita, L. Mwambarangwe, S. L. Braunstein, J. van de Wijgert, R. Sahabo, J. E. Justman, W. El-Sadr, and S. K. Sia, "Microfluidics-based diagnostics of infectious diseases in the developing world," *Nature Medicine*, vol. 17, pp. 1015–1019, jul 2011.

[139] W. R. Rodriguez, N. Christodoulides, P. N. Floriano, S. Graham, S. Mohanty, M. Dixon, M. Hsiang, T. Peter, S. Zavahir, I. Thior, D. Romanovicz, B. Bernard, A. P. Goodey, B. D. Walker, and J. T. McDevitt, "A Microchip CD4 Counting Method for HIV Monitoring in Resource-Poor Settings," *PLoS Medicine*, vol. 2, p. e182, jul 2005.

[140] L. Mazutis, J. Gilbert, W. L. Ung, D. A. Weitz, A. D. Griffiths, and J. A. Heyman, "Single-cell analysis and sorting using droplet-based microfluidics," *Nature Protocols*, vol. 8, pp. 870–891, apr 2013.

[141] H.-Y. Wang and C. Lu, "High-throughput and real-time study of single cell electroporation using microfluidics: Effects of medium osmolarity," *Biotechnology and Bioengineering*, vol. 95, pp. 1116–1125, dec 2006.

[142] S. Chung, R. Sudo, P. J. Mack, C.-R. Wan, V. Vickerman, and R. D. Kamm, "Cell migration into scaffolds under co-culture conditions in a microfluidic platform," *Lab Chip*, vol. 9, no. 2, pp. 269–275, 2009.

[143] K. Ziółkowska, A. Stelmachowska, R. Kwapiszewski, M. Chudy, A. Dybko, and Z. Brzózka, "Long-term three-dimensional cell culture and anticancer drug activity evaluation in a microfluidic chip," *Biosensors and Bioelectronics*, vol. 40, no. 1, pp. 68–74, 2013.

[144] M. A. McClain, C. T. Culbertson, S. C. Jacobson, and J. M. Ramsey, "Flow cytometry of Escherichia coli on microfluidic devices," *Analytical Chemistry*, vol. 73, no. 21, pp. 5334–5338, 2001.

[145] M. Wu, M. Piccini, C.-Y. Koh, K. S. Lam, and A. K. Singh, "Single Cell MicroRNA Analysis Using Microfluidic Flow Cytometry," *PLoS ONE*, vol. 8, p. e55044, jan 2013.

[146] S. C. Hur, N. K. Henderson-MacLennan, E. R. B. McCabe, and D. Di Carlo, "Deformability-based cell classification and enrichment using inertial microfluidics," *Lab on a Chip*, vol. 11, no. 5, p. 912, 2011.

[147] X. Li, W. Chen, G. Liu, W. Lu, and J. Fu, "Continuous-flow microfluidic blood cell sorting for unprocessed whole blood using surface-micromachined microfiltration membranes," *Lab on a Chip*, vol. 14, no. 14, p. 2565, 2014.

[148] S. Xu, Z. Nie, M. Seo, P. Lewis, E. Kumacheva, H. A. Stone, P. Garstecki, D. B. Weibel, I. Gitlin, and G. M. Whitesides, "Generation of Monodisperse Particles by Using Microfluidics: Control over Size, Shape, and Composition," *Angewandte Chemie*, vol. 117, pp. 734–738, jan 2005.

[149] C.-C. Lee, G. Sui, A. Elizarov, C. J. Shu, Y.-S. Shin, A. N. Dooley, J. Huang, A. Daridon, P. Wyatt, D. Stout, H. C. Kolb, O. N. Witte, N. Satyamurthy, J. R. Heath, M. E. Phelps, S. R. Quake, and H.-R. Tseng, "Multistep Synthesis of a Radiolabeled Imaging Probe Using Integrated Microfluidics," *Science*, vol. 310, no. 5755, 2005.

[150] B. Henrik, "Theoretical microfluidics," *MIC-Department of micro and Nanotechnology, Technical University of Denmark*, vol. 2, 2005.

[151] A. Ainla, G. Jeffries, and A. Jesorka, "Hydrodynamic flow confinement technology in microfluidic perfusion devices," *Micromachines*, vol. 3, no. 2, pp. 442–461, 2012.

[152] N. S. Veselovsky, F. Engert, and H. D. Lux, "Fast local superfusion technique," *Pflugers Archiv European Journal of Physiology*, vol. 432, pp. 351–354, jun 1996.

[153] T. Bonhoeffer and F. Engert, "Synapse specificity of long-term potentiation breaks down at short distances," *Nature*, vol. 388, pp. 279–284, jul 1997.

[154] C. Lohmann, A. Finski, and T. Bonhoeffer, "Local calcium transients regulate the spontaneous motility of dendritic filopodia," *Nature Neuroscience*, vol. 8, pp. 305–312, mar 2005.

[155] O. Feinerman and E. Moses, "A picoliter 'fountain-pen' using co-axial dual pipettes," *Journal of Neuroscience Methods*, vol. 127, no. 1, pp. 75–84, 2003.

[156] D. Juncker, H. Schmid, and E. Delamarche, "Multipurpose microfluidic probe," *Nature Materials*, vol. 4, pp. 622–628, aug 2005.

[157] G. V. Kaigala, R. D. Lovchik, U. Drechsler, and E. Delamarche, "A Vertical Microfluidic Probe," *Langmuir*, vol. 27, pp. 5686–5693, may 2011.

[158] Y. L. Han, J. Hu, G. M. Genin, T. J. Lu, and F. Xu, "BioPen: direct writing of functional materials at the point of care.," *Scientific reports*, vol. 4, p. 4872, jan 2014.

[159] D. Chen, W. Du, Y. Liu, W. Liu, A. Kuznetsov, F. E. Mendez, L. H. Philipson, and R. F. Ismagilov, "The chemistrode: a droplet-based microfluidic device for stimulation and recording with high temporal, spatial, and chemical resolution.," *Proceedings of the National Academy of Sciences of the United States of America*, vol. 105, no. 44, pp. 16843–16848, 2008.

[160] D. Momotenko, F. Cortes-Salazar, A. Lesch, G. Wittstock, and H. H. Girault, "Microfluidic Push–Pull Probe for Scanning Electrochemical Microscopy," *Analytical Chemistry*, vol. 83, pp. 5275–5282, jul 2011.

[161] A. Ainla, G. D. M. Jeffries, R. Brune, O. Orwar, and A. Jesorka, "A multifunctional pipette," *Lab on a Chip*, vol. 12, no. 7, p. 1255, 2012.

[162] S. Lehnert, *Biomolecular action of ionizing radiation*. CRC Press, 2007.

[163] P. Siegel, "Terahertz technology," *IEEE Transactions on Microwave Theory and Techniques*, vol. 50, pp. 910–928, mar 2002.

[164] P. Planken and H. Bakker, "Towards time-resolved THz imaging," *Applied Physics A: Materials Science & Processing*, vol. 78, pp. 465–469, mar 2004.

[165] N. C. J. van der Valk, W. A. M. van der Marel, and P. C. M. Planken, "Terahertz polarization imaging," *Optics Letters*, vol. 30, no. 20, p. 2802, 2005.

[166] A. Hirata, T. Kosugi, H. Takahashi, R. Yamaguchi, F. Nakajima, T. Furuta, H. Ito, H. Sugahara, Y. Sato, and T. Nagatsuma, "120-GHz-band millimeter-wave photonic wireless link for 10-Gb/s data transmission," *IEEE Transactions on Microwave Theory and Techniques*, vol. 54, pp. 1937–1944, may 2006.

[167] K. Ishigaki, M. Shiraishi, S. Suzuki, M. Asada, N. Nishiyama, and S. Arai, "Direct intensity modulation and wireless data transmission characteristics of terahertz-oscillating resonant tunnelling diodes," *Electronics Letters*, vol. 48, no. 10, p. 582, 2012.

[168] R. M. Woodward, B. E. Cole, V. P. Wallace, R. J. Pye, D. D. Arnone, E. H. Linfield, and M. Pepper, "Terahertz pulse imaging in reflection geometry of human skin cancer and skin tissue," *Physics in medicine and biology*, vol. 47, pp. 3853–63, nov 2002.

[169] S. M. Kim, F. Hatami, J. S. Harris, A. W. Kurian, J. Ford, D. King, G. Scalari, M. Giovannini, N. Hoyler, J. Faist, and G. Harris, "Biomedical terahertz imaging with a quantum cascade laser," *Applied Physics Letters*, vol. 88, no. 15, p. 153903, 2006.

[170] P. Tewari, C. P. Kealey, D. B. Bennett, N. Bajwa, K. S. Barnett, R. S. Singh, M. O. Culjat, A. Stojadinovic, W. S. Grundfest, and Z. D. Taylor, "In vivo terahertz imaging of rat skin burns," *Journal of Biomedical Optics*, vol. 17, no. 4, p. 040503, 2012.

[171] I. V. Lundholm, H. Rodilla, W. Y. Wahlgren, A. Duelli, G. Bourenkov, J. Vukusic, R. Friedman, J. Stake, T. Schneider, and G. Katona, "Terahertz radiation induces non-thermal structural changes associated with Fröhlich condensation in a protein crystal," *Structural Dynamics*, vol. 2, p. 054702, sep 2015.

[172] J. Xu, K. W. Plaxco, and S. J. Allen, "Probing the collective vibrational dynamics of a protein in liquid water by terahertz absorption spectroscopy.," *Protein Science*, vol. 15, pp. 1175–81, may 2006.

[173] R. J. Falconer and A. G. Markelz, "Terahertz Spectroscopic Analysis of Peptides and Proteins," *Journal of Infrared, Millimeter, and Terahertz Waves*, vol. 33, pp. 973–988, oct 2012.

[174] B. M. Fischer, M. Hoffmann, H. Helm, R. Wilk, F. Rutz, T. Kleine-Ostmann, M. Koch, and P. U. Jepsen, "Terahertz time-domain spectroscopy and imaging of artificial RNA," *Optics Express*, vol. 13, no. 14, p. 5205, 2005.

[175] A. Ramundo Orlando and G. P. Gallerano, "Terahertz radiation effects and biological applications," *Journal of Infrared, Millimeter, and Terahertz Waves*, vol. 30, no. 12, pp. 1308–1318, 2009.

[176] M. Tonouchi, "Cutting-edge terahertz technology," *Nature Photonics*, vol. 1, pp. 97–105, feb 2007.

[177] P. H. Siegel, "Terahertz technology in biology and medicine," *IEEE Transactions on Microwave Theory and Techniques*, vol. 52, no. 10, pp. 2438–2447, 2004.

[178] A. Amirudin and D. Thieny, "Application of electrochemical impedance spectroscopy to study the degradation of polymer-coated metals," 1995.

[179] J. Pan, D. Thierry, and C. Leygraf, "Electrochemical impedance spectroscopy study of the passive oxide film on titanium for implant application," *Electrochimica Acta*, vol. 41, no. 7, pp. 1143–1153, 1996.

[180] Qing Wang, , Jacques-E. Moser, and M. Grätzel*, "Electrochemical Impedance Spectroscopic Analysis of Dye-Sensitized Solar Cells," *J. Phys. Chem. B*, vol. 109, no. 31, pp. 1495–14953, 2005.

[181] K. Jüttner, "Electrochemical impedance spectroscopy (EIS) of corrosion processes on inhomogeneous surfaces," *Electrochimica Acta*, vol. 35, no. 10, pp. 1501–1508, 1990.

[182] B. Ge, T. Meyer, M. Schöning, U. Wollenberger, and F. Lisdat, "Cytochrome c' from Chromatium vinosum on gold electrodes." 2000.

[183] A. Angersbach, V. Heinz, and D. Knorr, "Evaluation of Process-Induced Dimensional Changes in the Membrane Structure of Biological Cells Using Impedance Measurement," *Biotechnology Progress*, vol. 18, pp. 597–603, jun 2002.

[184] E. Du, S. Ha, M. Diez-Silva, M. Dao, S. Suresh, and A. P. Chandrakasan, "Electric impedance microflow cytometry for characterization of cell disease states," *Lab on a Chip*, vol. 13, no. 19, p. 3903, 2013.

[185] J. Guo, C. M. Li, and Y. Kang, "PDMS-film coated on PCB for AC impedance sensing of biological cells," *Biomedical Microdevices*, vol. 16, pp. 681–686, oct 2014.

[186] K. Grenier, D. Dubuc, T. Chen, F. Artis, T. Chretiennot, M. Poupot, and J. J. Fournie, "Recent advances in microwave-based dielectric spectroscopy at the cellular level for cancer investigations," *IEEE Transactions on Microwave Theory and Techniques*, vol. 61, no. 5, pp. 2023–2030, 2013.

[187] Y.-F. Chen, H.-W. Wu, Y.-H. Hong, and H.-Y. Lee, "40 GHz RF biosensor based on microwave coplanar waveguide transmission line for cancer cells (HepG2) dielectric characterization," *Biosensors and Bioelectronics*, vol. 61, pp. 417–421, 2014.

[188] M. Olapinski, S. Manus, M. George, A. Brüggemann, N. Fertig, and F. C. Simmel, "Detection of lipid bilayer and peptide pore formation at gigahertz frequencies," *Applied Physics Letters*, vol. 88, no. 2006, p. 13902, 2006.

[189] S. Liu, S. Member, I. Ocket, and M. Cauwe, "Sensitivity Analysis of Broadband On-Wafer Dielectric Spectroscopy of Yeast Cell Suspensions up to 110 GHz," *IEEE Microwave and Wireless Components Letters*, vol. 25, no. 3, pp. 199–201, 2015.

[190] C. Wen, "Coplanar Waveguide: A Surface Strip Transmission Line Suitable for Nonreciprocal Gyromagnetic Device Applications," *IEEE Transactions on Microwave Theory and Techniques*, vol. 17, pp. 1087–1090, dec 1969.

[191] H. Wheeler, "Transmission-Line Properties of Parallel Strips Separated by a Dielectric Sheet," *IEEE Transactions on Microwave Theory and Techniques*, vol. 13, pp. 172–185, mar 1965.

[192] H. Stinehelfer, "An Accurate Calculation of Uniform Microstrip Transmission Lines," *IEEE Transactions on Microwave Theory and Techniques*, vol. 16, pp. 439–444, jul 1968.

[193] G. Goubau, "Surface Waves and Their Application to Transmission Lines," *Journal of Applied Physics*, vol. 21, no. 11, p. 1119, 1950.

[194] G. A. Ferrier, S. F. Romanuik, D. J. Thomson, G. E. Bridges, and M. R. Freeman, "A microwave interferometric system for simultaneous actuation and detection of single biological cells," *Lab on a Chip*, vol. 9, no. 23, p. 3406, 2009.

[195] A. Treizebre, T. Akalin, and B. Bocquet, "Planar excitation of Goubau Transmission Lines for THz BioMEMS," *IEEE Microwave and Wireless Components Letters*, vol. 15, pp. 886–888, dec 2005.

[196] M. Nordin and T. Laurell, "Two-hundredfold volume concentration of dilute cell and particle suspensions using chip integrated multistage acoustophoresis," *Lab on a Chip*, vol. 12, no. 22, p. 4610, 2012.

[197] M. Tenje, M. N. Lundgren, A.-M. Swärd-Nilsson, J. Kjeldsen-Kragh, L. Lyxe, and A. Lenshof, "Acoustophoretic removal of proteins from blood components," *Biomedical Microdevices*, vol. 17, p. 95, oct 2015.

[198] J. Dykes, A. Lenshof, I.-B. Åstrand-Grundström, T. Laurell, and S. Scheding, "Efficient Removal of Platelets from Peripheral Blood Progenitor Cell Products Using a Novel Micro-Chip Based Acoustophoretic Platform," *PLoS ONE*, vol. 6, p. e23074, aug 2011.

[199] A. H. Ng, M. Lee, K. Choi, A. T. Fischer, J. M. Robinson, and A. R. Wheeler, "Digital Microfluidic Platform for the Detection of Rubella Infection and Immunity: A Proof of Concept," *Clinical Chemistry*, vol. 61, no. 2, 2015.

[200] S. C. Shih, I. Barbulovic-Nad, X. Yang, R. Fobel, and A. R. Wheeler, "Digital microfluidics with impedance sensing for integrated cell culture andanalysis," *Biosensors and Bioelectronics*, vol. 42, pp. 314–320, 2013.

[201] X. Liang and S. Y. Chou, "Nanogap Detector Inside Nanofluidic Channel for Fast Real-Time Label-Free DNA Analysis," *Nano Letters*, vol. 8, pp. 1472–1476, may 2008.

[202] W. Reisner, N. B. Larsen, A. Silahtaroglu, A. Kristensen, N. Tommerup, J. O. Tegenfeldt, and H. Flyvbjerg, "Single-molecule denaturation mapping of DNA in nanofluidic channels.," *Proceedings of the National Academy of Sciences of the United States of America*, vol. 107, pp. 13294–9, jul 2010.

[203] J. Fu, R. B. Schoch, A. L. Stevens, S. R. Tannenbaum, and J. Han, "A patterned anisotropic nanofluidic sieving structure for continuous-flow separation of DNA and proteins," *Nature Nanotechnology*, vol. 2, pp. 121–128, feb 2007.

[204] R. Karnik, K. Castelino, and A. Majumdar, "Field-effect control of protein transport in a nanofluidic transistor circuit," *Applied Physics Letters*, vol. 88, no. 12, p. 123114, 2006.

[205] N. Chronis, M. Zimmer, and C. I. Bargmann, "Microfluidics for in vivo imaging of neuronal and behavioral activity in Caenorhabditis elegans.," *Nature methods*, vol. 4, pp. 727–31, sep 2007.

[206] E. M. Lucchetta, J. H. Lee, L. A. Fu, N. H. Patel, and R. F. Ismagilov, "Dynamics of Drosophila embryonic patterning network perturbed in space and time using microfluidics," *Nature*, vol. 434, pp. 1134–1138, apr 2005.

[207] M. Ghannad-Rezaie, X. Wang, B. Mishra, C. Collins, and N. Chronis, "Microfluidic Chips for In Vivo Imaging of Cellular Responses to Neural Injury in Drosophila Larvae," *PLoS ONE*, vol. 7, p. e29869, jan 2012.